

Alma Mater Studiorum Università di Bologna  
Archivio istituzionale della ricerca

Equivalence of two diagram representations of links in lens spaces and essential invariants

This is the final peer-reviewed author's accepted manuscript (postprint) of the following publication:

*Published Version:*

Cattabriga, A., Manfredi, E., Rigolli, L. (2015). Equivalence of two diagram representations of links in lens spaces and essential invariants. ACTA MATHEMATICA HUNGARICA, 146(1), 168-201 [10.1007/s10474-015-0475-z].

*Availability:*

This version is available at: <https://hdl.handle.net/11585/551457> since: 2016-07-13

*Published:*

DOI: <http://doi.org/10.1007/s10474-015-0475-z>

*Terms of use:*

Some rights reserved. The terms and conditions for the reuse of this version of the manuscript are specified in the publishing policy. For all terms of use and more information see the publisher's website.

This item was downloaded from IRIS Università di Bologna (<https://cris.unibo.it/>).  
When citing, please refer to the published version.

(Article begins on next page)

This is the final peer-reviewed accepted manuscript of:

**Cattabriga, A., Manfredi, E. & Rigolli, L. Equivalence of two diagram representations of links in lens spaces and essential invariants. *Acta Math. Hungar.* 146, 168–201 (2015).**

The final published version is available online at : <https://doi.org/10.1007/s10474-015-0475-z>

Rights / License:

The terms and conditions for the reuse of this version of the manuscript are specified in the publishing policy. For all terms of use and more information see the publisher's website.

*This item was downloaded from IRIS Università di Bologna (<https://cris.unibo.it/>)*

***When citing, please refer to the published version.***

# Equivalence of two diagram representations of links in lens spaces and essential invariants \*

Alessia Cattabriga, Enrico Manfredi, Lorenzo Rigolli

October 30, 2018

## Abstract

In this paper we study the relation between two diagrammatic representations of links in lens spaces: the disk diagram introduced in [CMM] and the grid diagram introduced in [BGH, Co] and we find how to pass from one to the other. We also investigate whether the HOMFLY-PT invariant and the Link Floer Homology are essential invariants, that is, we try to understand if these invariants are able to distinguish links in  $L(p, q)$  covered by the same link in  $\mathbf{S}^3$ . In order to do so, we generalize the combinatorial definition of Knot Floer Homology in lens spaces developed in [BGH, MOS] to the case of links and we analyze how both the invariants change when we switch the orientation of the link.

*Mathematics Subject Classification 2010:* Primary 57R58, 57M27; Secondary 57M25.

*Keywords:* knots/links, lens spaces, lift, grid diagram, HOMFLY-PT polynomial, Link Floer Homology.

---

\*Work performed under the auspices of G.N.S.A.G.A. of C.N.R. of Italy and supported by M.U.R.S.T., by the University of Bologna, funds for selected research topics.

# 1 Introduction

For many years the study of knots and links has been confined to the case of  $\mathbf{S}^3$ , where different combinatorial representations as well as powerful invariants were developed in order to study the equivalence problem. In the last ten years, as far as the knowledge on 3-manifolds was improving, knot theory has shifted also to manifolds different from  $\mathbf{S}^3$ . In this setting, lens spaces play a leading role for many different reasons. For example some knots conjectures in  $\mathbf{S}^3$  can be rephrased in terms of links in lens spaces, as, for example, the Berge conjecture (see [Be1, Be2, Gr]). Furthermore there are interesting articles explaining applications of knots in lens spaces outside mathematics: [St] exploits them to describe topological string theories and [BM] uses them to describe the resolution of a biological DNA recombination problem. Another fundamental reason is that, among three manifolds, lens spaces are quite well understood. They are defined as finite cyclic quotient of  $\mathbf{S}^3$ , but they admit many different (combinatorial) representation that have been extended to represent also the links contained inside them. In [La, LR1, LR2] Dehn surgery representation of lens spaces is used to construct mixed link diagram, while in [CM] the representation of lens spaces as genus one Heegaard splitting leads to an algebraic representation of links in lens spaces using the elements of the mapping class group. The same representation of lens spaces is used in [BGH] to generalize to links in lens spaces the notion of grid diagram introduced in [Br, Cr, Dy] for the 3-sphere case, and used in [MOS] to describe a combinatorial version of the Link Floer Homology. Exploiting this representation, the authors manage to extend Knot Floer Homology to lens space, whereas in [Co] a HOMFLY-PT invariant is constructed. A disk diagram representation as well as Reidemeister type moves are introduced in [Dr, CMM] looking at lens spaces as the result of pasting a 3-ball along its boundary. Using this diagram, in [Dr, Mr] a Jones type polynomial and a HOMFLY and Kauffman skein modules are constructed for the case of  $L(2, 1) = \mathbb{RP}^3$ . This diagram is generalized to all lens spaces in [CMM], where the authors use it to compute the fundamental

group as well as the twisted Alexander polynomial. As far as so many invariant have been extended to links in lens spaces, a natural question arising is the following: which of them is able to distinguish different links in a certain lens space covered by the same link in  $\mathbf{S}^3$ ? Such an invariant is called *essential*. In [Ma1, Ma2] the author finds many examples of different links in the same lens space covered by the same link in  $\mathbf{S}^3$  and discuss the essentiality of some geometric invariants as the twisted Alexander polynomial. In this paper we analyze the case of the HOMFLY-PT invariant and the Link Floer Homology. In order to do so, we describe how to pass from a grid diagram representation to a disk diagram representation of the same link.

This paper is organized as follows. In section 2 we recall the definition of disk diagram and the corresponding Reidemeister type moves introduced in [CMM].

In Section 3, first we resume the definition of grid diagram introduced in [BGH, Co], then we find how to pass from a disk diagram of a given link  $L$  in  $L(p, q)$  to a grid diagram of the same link and vice versa. We also discuss the correspondence between Reidemeister type moves on the disk diagram and equivalence moves on the grid diagram.

In Section 4 we deal with the HOMFLY-PT invariant of links in lens spaces introduced in [Co]. We study how it behaves under change of orientation of the link and we compute it on some examples in order to discuss whether this invariant is essential or not.

Finally, Section 5 concerns Link Floer Homology. We generalize the combinatorial definition of Link Floer Homology, developed in [MOS] for links in  $\mathbf{S}^3$  and in [BGH] for knots in lens spaces, to the case of links in lens spaces and study its behaviour under change of orientation. We find examples of links with the same covering distinguished by this invariant. All the detailed computations of the Link Floer Homology of such examples are contained in the Appendix.

The results stated in this paper hold both in the *Diff* category and in the *PL* category, as well as in the *Top* category if we consider only tame links.

Moreover we consider oriented links up to ambient isotopy.

## 2 Links in lens spaces via disk diagrams

In this section we recall the notion of the disk diagram for links in lens spaces developed in [CMM], and the corresponding equivalence moves.

**A model for lens spaces** We start by recalling the model that we use for lens spaces. Let  $p$  and  $q$  be two coprime integers such that  $0 \leq q < p$ . The unit ball is the set  $B^3 = \{(x_1, x_2, x_3) \in \mathbb{R}^3 \mid x_1^2 + x_2^2 + x_3^2 \leq 1\}$  and  $E_+$  and  $E_-$  denote, respectively, the upper and the lower closed hemisphere of  $\partial B^3$ . Label with  $B_0^2$  the equatorial disk, that is the intersection of the plane  $x_3 = 0$  with  $B^3$ . Finally let  $N = (0, 0, 1)$  and  $S = (0, 0, -1)$ . Consider the rotation  $g_{p,q}: E_+ \rightarrow E_+$  of  $2\pi q/p$  radians around the  $x_3$ -axis and the reflection  $f_3: E_+ \rightarrow E_-$  with respect to the plane  $x_3 = 0$  (see Figure 1).

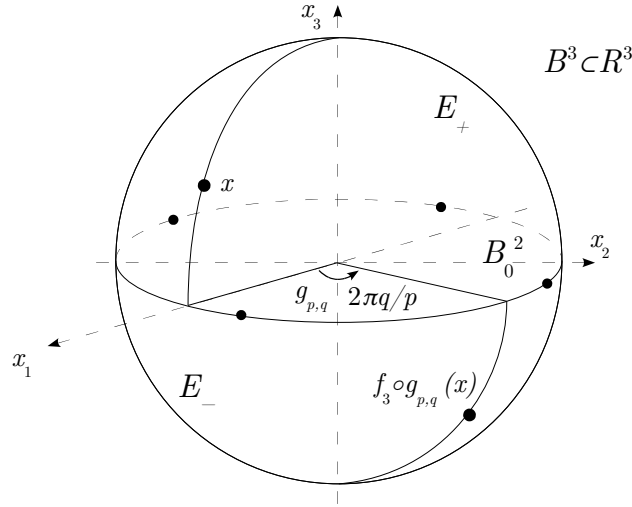


Figure 1: A model for  $L(p, q)$ .

The *lens space*  $L(p, q)$  is the quotient of  $B^3$  by the equivalence relation on  $\partial B^3$  which identifies  $x \in E_+$  with  $f_3 \circ g_{p,q}(x) \in E_-$ . We denote with  $F: B^3 \rightarrow L(p, q) = B^3 / \sim$  the quotient map. Notice that on the equator

$\partial B_0^2 = E_+ \cap E_-$  each equivalence class contains  $p$  points. Clearly we have  $L(1, 0) \cong \mathbf{S}^3$  and  $L(2, 1) \cong \mathbb{RP}^3$ .

**The construction of the disk diagram** We briefly recall the construction of the disk diagram for a link in a lens space developed in [CMM]. Throughout the section we assume  $p > 1$ . Let  $L \subset L(p, q)$  be a link and consider  $L' = F^{-1}(L)$ . By moving  $L$  via a small isotopy in  $L(p, q)$ , we can suppose that  $L'$  is the disjoint union of closed curves in  $\text{int}(B^3)$  and arcs properly embedded in  $B^3$  not containing  $N$  and  $S$ . Let  $\mathbf{p}: B^3 \setminus \{N, S\} \rightarrow B_0^2$  be the projection defined by  $\mathbf{p}(x) = c(x) \cap B_0^2$ , where  $c(x)$  is the circle (possibly a line) through  $N$ ,  $x$  and  $S$ . Project  $L'$  using  $\mathbf{p}|_{L'}: L' \rightarrow B_0^2$ .

As in the classical case, we can assume, by moving  $L$  via a small isotopy, that the projection  $\mathbf{p}|_{L'}: L' \rightarrow B_0^2$  of  $L$  is *regular*, namely

- (1) the projection of  $L'$  contains no cusps;
- (2) all auto-intersections of  $\mathbf{p}(L')$  are transversal;
- (3) the set of multiple points is finite, and all of them are actually double points;
- (4) no double point is on  $\partial B_0^2$ .

Finally, double points are resolved with underpasses and overpasses as in the diagram for links in  $\mathbf{S}^3$ . A *disk diagram* of a link  $L$  in  $L(p, q)$  is a regular projection of  $L' = F^{-1}(L)$  on the equatorial disk  $B_0^2$ , with specified overpasses and underpasses (see Figure 2).

Notice that an orientation of the link  $L$  induces an orientation on  $L'$  and so on a diagram of  $L$ .

In order to make the disk diagram more comprehensible, we add an indexation of the boundary points of the projection as follows: first, assume that the equator  $\partial B_0^2$  is oriented counterclockwise if we look at it from  $N$ , then, according to this orientation, label with  $+1, \dots, +t$  the endpoints of the projection of the link coming from the upper hemisphere, and with  $-1, \dots, -t$  the endpoints coming from the lower hemisphere, respecting the rule  $+i \sim -i$ . An example is shown in Figure 2.

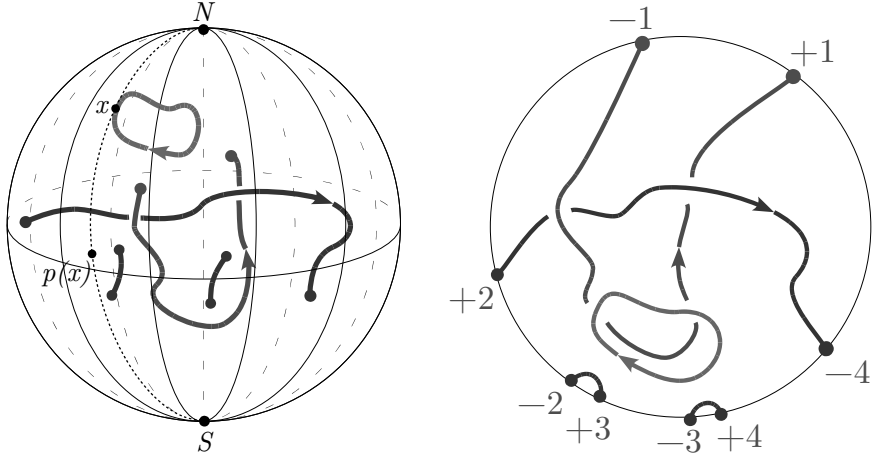


Figure 2: A link in  $L(9, 1)$  and its corresponding disk diagram.

**Reidemeister type moves** In [CMM] it is shown that two disk diagrams represent the same link if and only if they are connected by a finite sequence of the seven Reidemeister type moves depicted in Figure 3.

### 3 Connection with the grid diagram of links in lens space

In this section first we recall the notion of grid the diagram for links in lens spaces developed in [BGH] and [Co], then we explain how to transform a disk diagram into a grid diagram and vice versa, showing also the connection between the equivalence moves on the two different diagrams.

**Grid diagram of links in lens space** A (*toroidal*) *grid diagram*  $G$  in  $L(p, q)$  with grid number  $n$  is a quintuple  $(T^2, \alpha, \beta, \mathbb{O}, \mathbb{X})$  that satisfies the following conditions (see Figure 4 for an example with grid number 3 in  $L(4, 1)$ )

- $T^2$  is the standard oriented torus  $\mathbb{R}^2/\mathbb{Z}^2$ , where  $\mathbb{Z}^2$  is the lattice generated by the vectors  $(1, 0)$  and  $(0, 1)$ ;



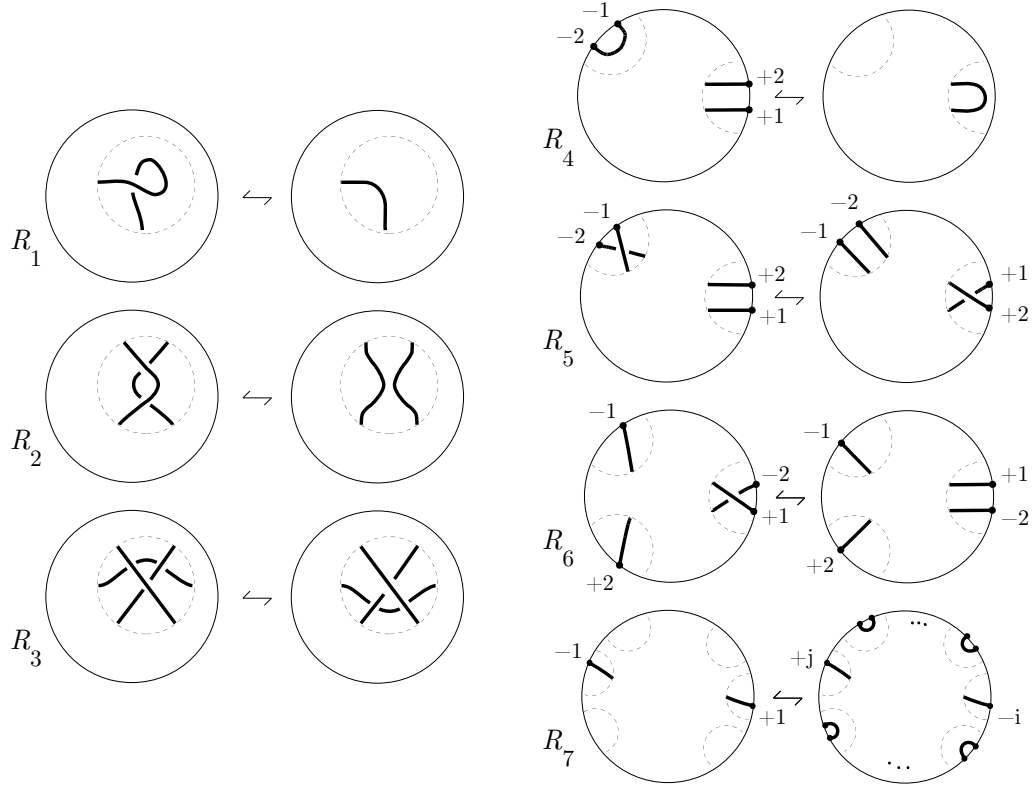


Figure 3: Generalized Reidemeister moves.

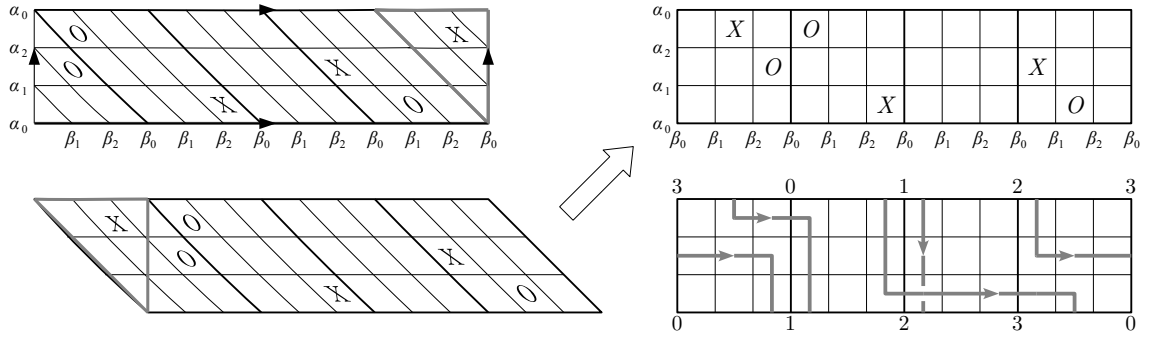


Figure 4: From a grid diagram with grid number 3 to its corresponding link in  $L(4, 1)$ .

- $\alpha = \{\alpha_0, \dots, \alpha_{n-1}\}$  are the images in  $T^2$  of the  $n$  lines in  $\mathbb{R}^2$  described by the equations  $y = i/n$ , for  $i = 0, \dots, n-1$ ; the complement  $T^2 \setminus (\alpha_0 \cup \dots \cup \alpha_{n-1})$  has  $n$  connected annular components, called the *rows* of the grid diagram;
- $\beta = \{\beta_0, \dots, \beta_{n-1}\}$  are the images in  $T^2$  of the  $n$  lines in  $\mathbb{R}^2$  described by the equations  $y = -\frac{p}{q}(x - \frac{i}{pn})$ , for  $i = 0, \dots, n-1$ ; the complement  $T^2 \setminus (\beta_0 \cup \dots \cup \beta_{n-1})$  has  $n$  connected annular components, called the *columns* of the grid diagram;
- $\mathbb{O} = \{O_0, \dots, O_{n-1}\}$  (resp.  $\mathbb{X} = \{X_0, \dots, X_{n-1}\}$ ) are  $n$  points in  $T^2 \setminus (\alpha \cup \beta)$  called *markings*, such that any two points in  $\mathbb{O}$  (resp.  $\mathbb{X}$ ) lie in different rows and in different columns.

In order to make the identifications of the diagram's boundary easier to understand, it is possible to perform the “shift” depicted in Figure 4. Notice that, if we forget about  $L(p, q)$ 's identifications, the curve  $\beta_0$  divides the rectangle of a grid diagram into  $p$  adjacent squares, that we will call *boxes* of the diagram.

A grid diagram  $G$  represents an oriented link  $L \subset L(p, q)$  obtained as follows. First, denote with  $V_\alpha$  and  $V_\beta$  the two solid tori having, respectively,  $\alpha$  and  $\beta$  as meridians. Clearly  $V_\alpha \cup_{T^2} V_\beta$  is a genus one Heegaard splitting representing  $L(p, q)$ . Then connect

- (1) each  $X_i$  to the unique  $O_j$  lying in the same row with an arc embedded in the row and disjoint from the curves of  $\alpha$ , and
- (2) each  $O_j$  to the unique  $X_l$  lying in the same column by an arc embedded in the column and disjoint from the curves of  $\beta$ ,

obtaining a multicurve immersed in  $T^2$ . Finally remove the self-intersections, pushing the lines of (1) into  $V_\alpha$  and the lines of (2) into  $V_\beta$ . The orientation on  $L$  is obtained by orienting the horizontal arcs connecting the markings from the  $X$  to the  $O$ . See Figure 4 for an example in  $L(4, 1)$ .

Notice that, the presence in the grid diagram of an pair of marking  $X$  and  $O$  in the same position corresponds to a trivial component of the represented link (see the bottom row of the first box of Figure 10).

By Theorem 4.3 of [BGH], each link  $L \subset L(p, q)$  can be represented by a grid diagram. The idea of the proof is a PL-approximation with orthogonal lines of the link projection on the torus.

**Equivalence moves for grid diagrams** A *grid (de)stabilization* is a move that (decreases) increases by one the grid number. Figure 5 shows an example in  $L(5, 2)$  of a  $X : NW$  grid (de)stabilization, where  $X$  is the grid marking chosen for the stabilization and  $NW$  refers to the arrangement of the new markings. Of course, we can have also (de)stabilization with respect to  $O$  markings and with  $NE, SW$  and  $SE$  arrangements.



Figure 5: An example of (de)stabilization in  $L(5, 2)$ .

A grid diagram *commutation* interchanges either two adjacent columns or two adjacent rows as follows. Let  $A$  be the annulus containing the two considered columns (or rows)  $c_1$  and  $c_2$ . The annulus is divided into  $pn$  parts by the rows (columns). Let  $s_1$  and  $s_2$  be the two bands of the annulus containing the markings of  $c_1$ . Then the commutation is *interleaving* if the markings of  $c_2$  are in different components of  $A - s_1 - s_2$ , and *non-interleaving* otherwise (see Figure 6).

**Proposition 1.** [BG] *Two grid diagrams of links in  $L(p, q)$  represent the same link if and only if there exists a finite sequence of (de)stabilizations and non-interleaving commutations connecting the two grid diagrams.*

Please notice that there are also two other hidden moves on a grid diagram, depending directly on the projection of the link on the Heegaard torus:



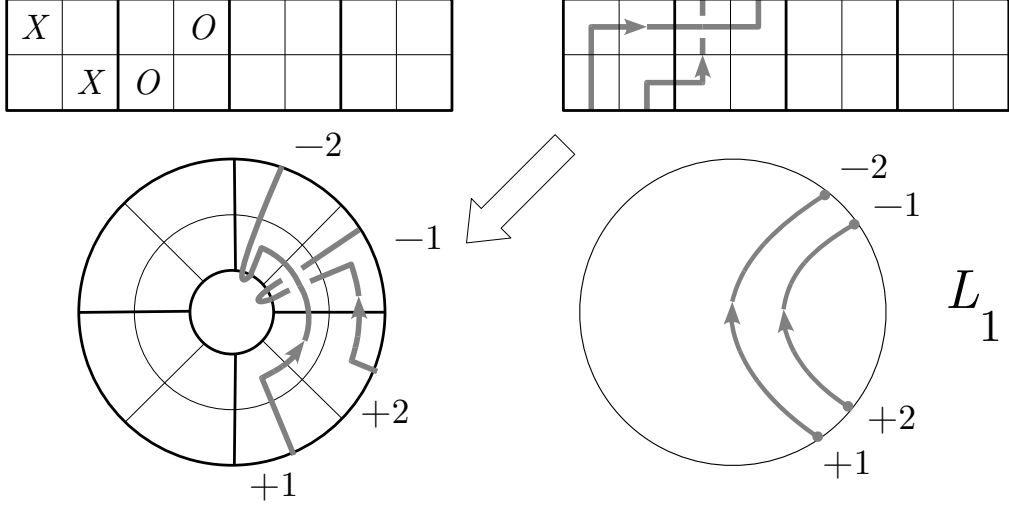


Figure 7: From grid diagram  $G_L$  to disk diagram  $D_L$  in  $L(4,1)$ .

is the toric Heegaard surface. If we want to transform the grid diagram into the disk diagram  $D_L$  we have to put our Heegaard surface inside  $B^3$  in the model of  $L(p,q)$  where we quotient  $B^3$  by the relation  $\sim$  on its boundary. This can be done as Figure 8 shows.

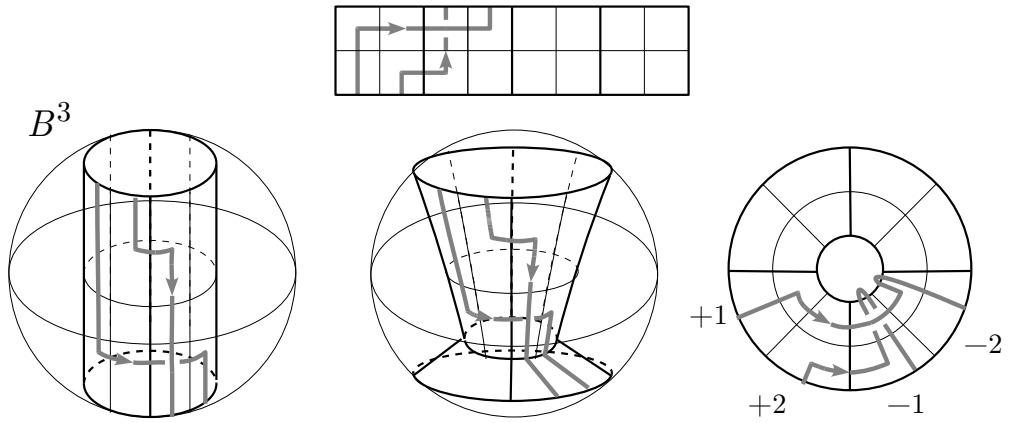


Figure 8: How to insert the grid diagram of  $L$  into the  $B^3$ -model of  $L(4,1)$ .

Now we want to project this surface on the equatorial disk  $B_0^2$ , and, in order to have a regular projection of the link, we deform the Heegaard torus as in Figure 8. The projection of the deformed grid diagram on  $B_0^2$  gives  $D_L$ .  $\square$

*Remark 3.* If the grid diagram  $G_L$  has grid number  $n$ , then the disk diagram  $D_L$ , obtained from  $G_L$ , has at most  $n(p-1)$  boundary points. Indeed, the number of boundary points of  $D_L$  is exactly the number of the points onto the lower and upper boundary of the rectangle of  $G_L$ , that is, at most,  $n(p-1)$ .

In the opposite direction, when we know the disk diagram  $D_L$  of a link  $L \subset L(p, q)$ , how can we recover the grid diagram  $G_L$ ?

**Proposition 4.** *Let  $L$  be a link in  $L(p, q)$ , defined by a disk diagram  $D_L$ , then we can get a grid diagram  $G_L$  of  $L$  as follows (see Figure 9)*

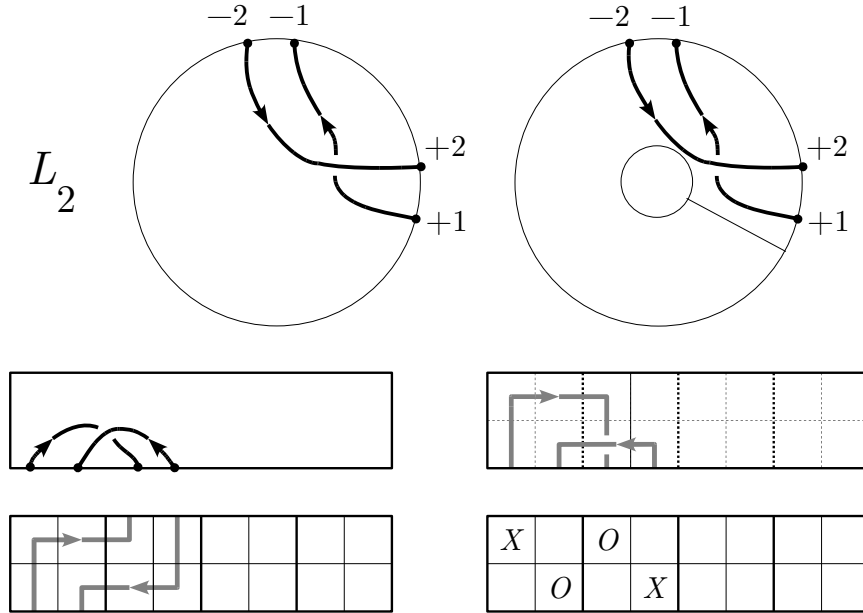


Figure 9: From disk diagram  $D_L$  to grid diagram  $G_L$  in  $L(4, 1)$ .

- consider the disk diagram  $D_L$  and cut the disk along a ray between the  $+1$  point and the previous boundary point (according to the orientation

of the disk), obtaining a rectangle;

- make an orthogonal PL-approximation of the link's arcs, putting all the crossings with horizontal overpass and vertical underpass;
- shift the boundary endpoint of  $-1, \dots, -t$  from the lower to the upper side of the rectangle, passing under all the lines;
- put  $X$  and  $O$  markings on the square corners of the link projection.

*Proof.* It is exactly the converse of the proof of Proposition 7. The only difference is that here we have to use the orthogonal PL-approximation suggested by Theorem 4.3 of [BGH].  $\square$

Using Propositions 2 and 4, it is possible to find also a correspondence between the Reidemeister moves on the disk diagrams (depicted in Figure 3) and the grid diagram's equivalence moves described in the previous paragraph. This correspondence is summed up in Table 3.

Disk diagram	Grid diagram
$R_1$	(de)stab.
$R_2$	non-inter. comm.
$R_3$	non-inter. comm.
$R_4$	cyclic perm. of rows
$R_5$	cyclic perm. of rows
$R_6$	non-inter. comm.
$R_7$	column reverse connection

## 4 Essential invariants: the HOMFLY-PT polynomial

In this section we deal with the HOMFLY-PT polynomial developed in [Co] in order to understand if it is an essential invariant, that is if it is able

to distinguish links covered by the same link in  $\mathbf{S}^3$ . We start by recalling its definition (see [Co] for the details).

We say that a link in  $L(p, q)$  is *trivial* if it can be represented by a grid diagram satisfying the following conditions

- the markings in each box lie only on the principal diagonal (the one going from NE-corner to the SW-corner);
- all the  $O$ -markings are contained in the the first box (from the left);
- the  $X$ -markings in the same box are contiguous, and if the first box contains  $X$ -markings, one of them lies in the SW corner;
- for each  $X$ -marking, all the other  $X$ -markings lying in a row below, must lie in a column on the left.

A trivial link will be denoted as  $U_{i_0, i_{p-1}, \dots, i_1}$  where  $i_j \in \mathbb{N}$  is the number of components of the link belonging to the  $j$ -th homology class. In Figure 10 is depicted the trivial link  $U_{1,0,1,2} \subset L(4, 1)$  having one 0-homologous component, zero 1-homologous component, one 2-homologous component and two 3-homologous components.

$O$								$X$									
	$O$				$X$												
		$O$				$X$											
			$\emptyset$														

Figure 10: Grid diagram for the trivial link  $U_{1,0,1,2}$  in  $L(4, 1)$ .

**Theorem 5.** [Co] *Let  $\mathcal{L}$  be the set of isotopy classes of links in  $L(p, q)$  and let  $\mathcal{TL} \subset \mathcal{L}$  denote the set of isotopy classes of trivial links. Define  $\mathcal{TL}^* \subset \mathcal{TL}$*



to be those trivial links with no nullhomologous components. Let  $U$  be the isotopy class of the standard unknot, a local knot in  $L(p, q)$  that bounds an embedded disk. Given a value  $J_{p,q}(T) \in \mathbb{Z}[a^{\pm 1}, z^{\pm 1}]$  for every  $T \in \mathcal{TL}^*$ , there is a unique map  $J_{p,q}: \mathcal{L} \rightarrow \mathbb{Z}[a^{\pm 1}, z^{\pm 1}]$  such that

- $J_{p,q}$  satisfies the skein relation  $a^{-p}J_{p,q}(L_+) - a^pJ_{p,q}(L_-) = zJ_{p,q}(L_0)$ .
- $J_{p,q}(U) = \left(\frac{a^{-1}-a}{z}\right)^{p-1}$
- $J_{p,q}(U \sqcup L) = \left(\frac{a^{-p}-a^p}{z}\right)J_{p,q}(L)$

As usual, the links  $L_+, L_-$ , and  $L_0$  differ only in a small neighborhood of a double point: Figure 11 shows how this difference appears on grid diagrams.

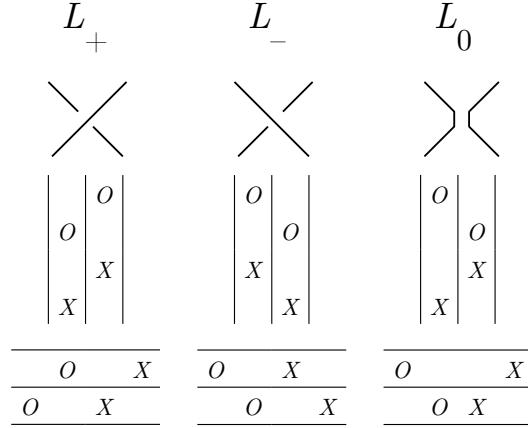


Figure 11: Grid skein relation.

The HOMFLY-PT invariant produced by Theorem 5 is not yet a polynomial, Cornwell suggests to produce a polynomial in the usual HOMFLY two variables by defining  $J_{p,q}$  on the trivial links as the classic HOMFLY-PT polynomial of their lift in the 3-sphere. Clearly, the essentiality of the HOMFLY-PT invariant depends on the assignment of a value to  $J_{p,q}$  on the class  $\mathcal{TL}^*$ : an assignment based on the lift makes the invariant much less sensitive in this direction.

**Behavior under change of orientation** What happens to the HOMFLY-PT invariant when we change the orientation of every component of the link? In the case of  $\mathbf{S}^3$ , the classic HOMFLY-PT polynomial does not change, but, in  $L(p, q)$  things are different since  $L(p, q)$  is homologically non-trivial.

**Proposition 6.** *Let  $L$  be a link in  $L(p, q)$  and denote with  $-L$  the link obtained by reversing the orientation of each component. If the HOMFLY-PT invariant of  $L$  can be written as  $J_{p,q}(L) = \sum a^k z^h J_{p,q}(U_{i_0, i_{p-1}, i_{p-2}, \dots, i_1})$ , then  $J_{p,q}(-L) = \sum a^k z^h J_{p,q}(U_{i_0, i_1, \dots, i_{p-2}, i_{p-1}})$ .*

*Proof.* As for the HOMFLY-PT polynomial for links in the 3-sphere, the skein reduction of both  $L$  and  $-L$  is the same, because if we change the orientation in  $L_+$ ,  $L_-$  and  $L_0$  we still get respectively  $L_+$ ,  $L_-$  and  $L_0$ . But if we change the orientation in the trivial links, then we find a different trivial link; more precisely, looking at Figure 12, if we change the orientation on the trivial link  $U_{i_0, i_{p-1}, i_{p-2}, \dots, i_1}$ , and perform at first a sequence of non-interleaving row commutations, then, a sequence of non-interleaving column commutations and finally some cyclic permutation of columns we obtain the trivial link  $U_{i_0, i_1, \dots, i_{p-2}, i_{p-1}}$ .  $\square$

Usually, in  $L(p, q)$ , the links  $L$  and  $-L$  are non equivalent (since they are generally homologically different). So, the last proposition suggests a way to construct examples of non-equivalent oriented links with the same lifting in  $\mathbf{S}^3$ , distinguished by the HOMFLY-PT invariant. Indeed it is enough to find a link  $L$  lifting to an invertible link and such that  $L$  is non isotopic to  $-L$ . For example, the knots  $K$  and  $-K$  in  $L(3, 1)$  in Figure 13 are different since the first one is 1-homologous whereas the second one is 2-homologous, but they both lift to the trivial knot in  $\mathbf{S}^3$ .

But what does it happen if the links with the same lift don't differ only from an orientation change? In [Ma1] the author finds many examples of different links in  $L(p, q)$  with the same covering in  $\mathbf{S}^3$ . We end the section by computing the HOMFLY-PT invariant of some of them. The first two examples are quite simple, since they are pairs of different trivial links: having

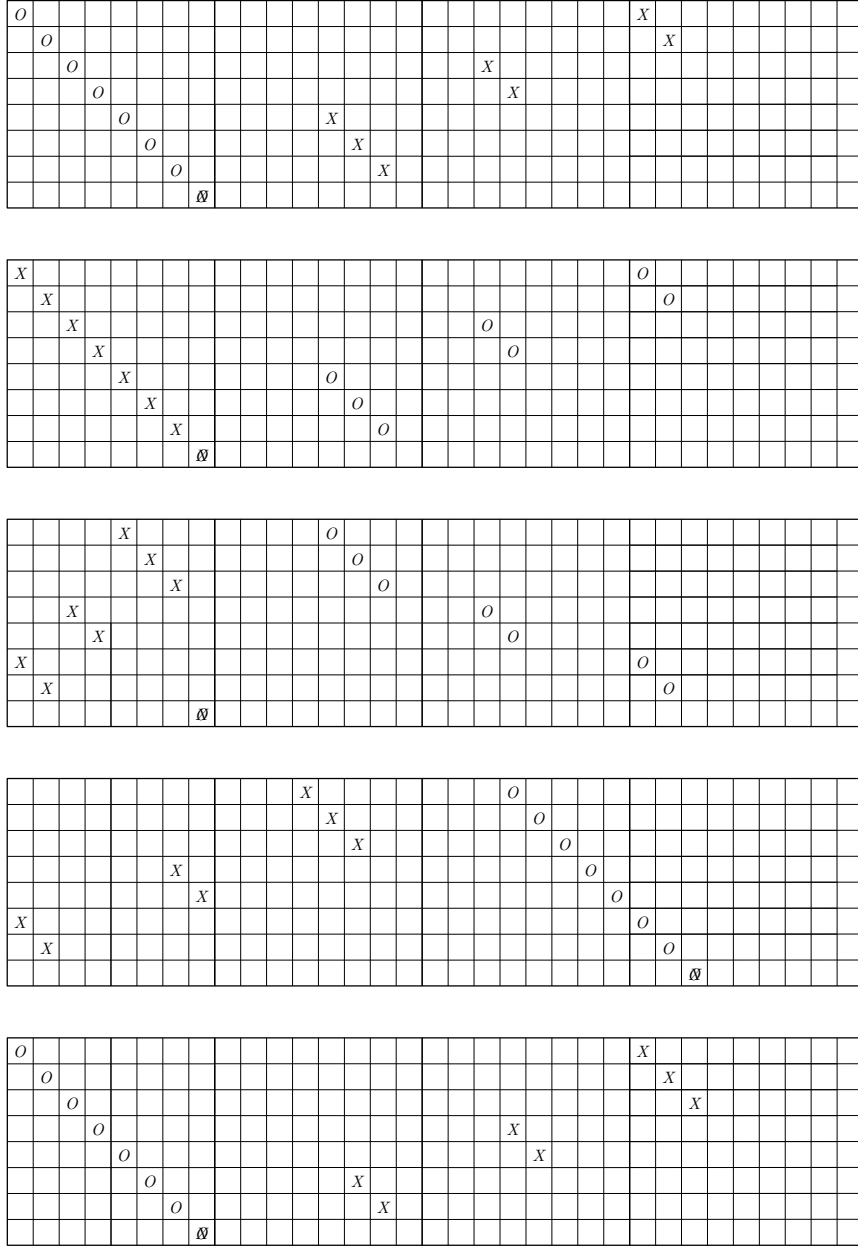


Figure 12: Reduction to trivial link of  $-U_{1,2,2,3}$  in  $L(4, 1)$ .

the same HOMFLY-PT invariant or not depends on how we define  $J_{p,q}$  on  $\mathcal{TL}^*$ . On the contrary, in the third example, that is much more complicated,

$$K \begin{array}{|c|c|c|} \hline O & & X \\ \hline \end{array} \quad \begin{array}{|c|c|c|} \hline X & & O \\ \hline O & X & \\ \hline \end{array} -K$$

Figure 13: Knots  $K$  and  $-K$  in  $L(3, 1)$  both lifting to the trivial knot in  $\mathbf{S}^3$ .

the two links are distinguished by the HOMFLY-PT polynomial.

**Example 7.** The two knots of Figure 14 are  $K_1$  and  $K_2$  in  $L(5, 2)$ . They are different since  $K_1$  is 1-homologous, while  $K_2$  is 2-homologous, but they both lift to the trivial knot in  $\mathbf{S}^3$  (see [Ma1]). Using Proposition 4, we get  $K_1 = U_{0,0,0,0,1}$  and  $K_2 = U_{0,0,0,1,0}$  in  $L(5, 2)$ . So, if we assume  $J_{p,q}(L) := J_{1,0}(\tilde{L})$  on trivial links, we clearly have  $J_{p,q}(K_1) = 1 = J_{p,q}(K_2)$ . It is possible to generalize this example to  $L(p, \frac{p \pm 1}{2})$  (see [Ma1]).

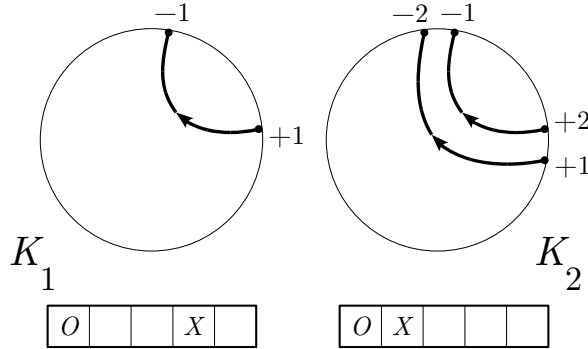


Figure 14: Diagrams for different knots in  $L(5, 2)$  with trivial lift.

**Example 8.** The two links  $L_A, L_B \subset L(4, 1)$  represented in Figure 15 are non-equivalent since the first one is a knot, whereas the second one is a two component link. Nevertheless, they both lift to the Hopf link in  $\mathbf{S}^3$  (see [Ma1]). Transforming the disk diagram into a grid diagram (see Proposition 4) and performing some destabilizations and non-interleaving commutations, we see that they are nothing else than the trivial links  $L_A = U_{0,0,1,0}$  and

$L_B = U_{0,1,0,1}$ . So, if we assume  $J_{p,q}(L) := J_{1,0}(\tilde{L})$  on trivial links, we clearly have  $J_{4,1}(L_A) = az + az^{-1} - a^3z^{-1} = J_{4,1}(L_B)$ .

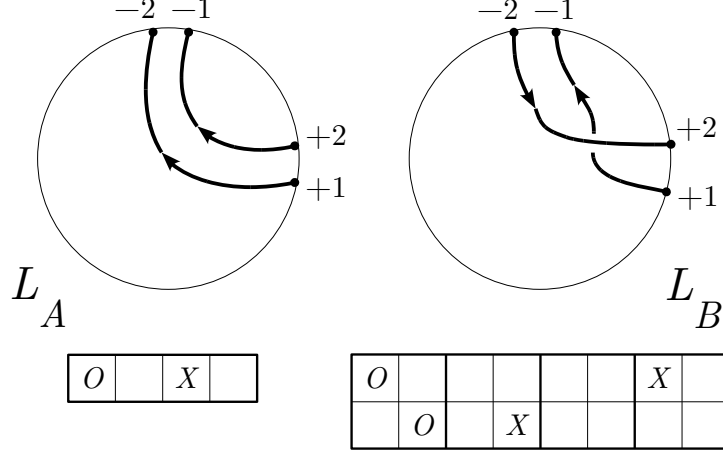


Figure 15: Diagrams for different links in  $L(4, 1)$  with Hopf link lift.

**Example 9.** The two links  $A_{2,2}$  and  $B_{2,2}$  in  $L(4, 1)$  depicted in Figure 16 are non equivalent, having different Alexander polynomial, but they both lift to the Hopf link in  $\mathbf{S}^3$  (see [Ma1]). The computation of their HOMFLY-PT invariant is very long. The skein reduction tree is quite big, so we report here only the final result

$$\begin{aligned}
J_{4,1}(A_{2,2}) &= (a^{24} + 3a^{24}z^2 + a^{24}z^4)J_{4,1}(U_{0,0,2,0}) + \\
&\quad + (3a^{28}z + 4a^{28}z^3 + a^{28}z^5)J_{4,1}(U_{1,0,0,0}) + \\
&\quad + (3a^{24}z^2 + 4a^{24}z^4 + a^{24}z^6)J_{4,1}(U_{0,1,0,1}) \\
J_{4,1}(B_{2,2}) &= (a^{24} + 2a^{24}z^2 + a^{24}z^4)J_{4,1}(U_{0,0,2,0}) + \\
&\quad + (a^{28}z + 2a^{28}z^3 + a^{28}z^5)J_{4,1}(U_{1,0,0,0}) + \\
&\quad + (a^{24}z^2 + 2a^{24}z^4 + a^{24}z^6)J_{4,1}(U_{0,1,0,1}) + \\
&\quad + (a^{20}z + 2a^{20}z^3)J_{4,1}(U_{0,2,1,0}) + \\
&\quad + a^{20}zJ_{4,1}(U_{0,0,1,2}) + a^{24}z^2J_{4,1}(U_{0,2,0,2}).
\end{aligned}$$

The lift of  $U_{0,1,0,1}$  is the Hopf link, the lift of  $U_{1,0,0,0}$  is the trivial link with four component and  $U_{0,2,1,0}$ ,  $U_{0,2,0,2}$ ,  $U_{0,0,1,2}$ ,  $U_{0,0,2,0}$  lif to the closure of the

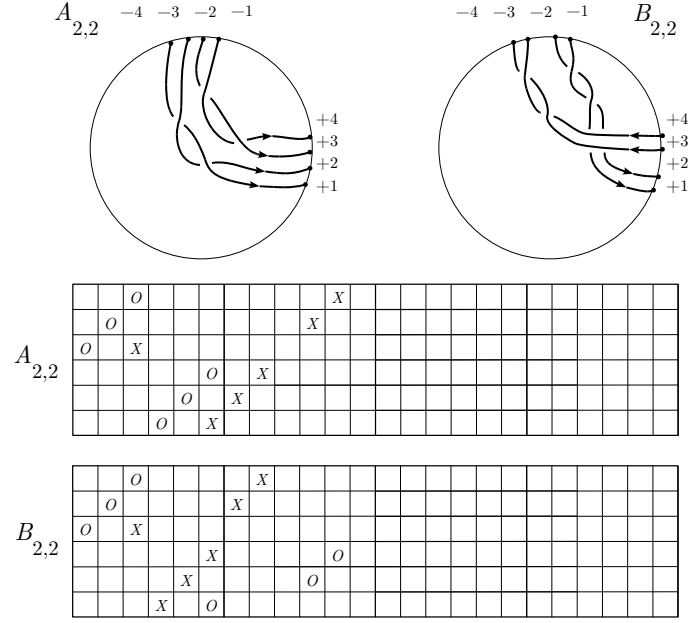


Figure 16: Grid diagrams for different links in  $L(4, 1)$  with Hopf link lift.

braid  $\Delta_4^2$ , where  $\Delta_4$  denotes the Garside braid on 4-strands (see [Ma1]). So, if we assume  $J_{4,1}(L) := J_{1,0}(\tilde{L})$  on trivial links, we get the following different HOMFLY-PT polynomials

$$\begin{aligned}
J_{4,1}(A_{2,2}) = & a^9 z^{-3} - 3a^{11} z^{-3} + 3a^{13} z^{-3} - a^{15} z^{-3} + 3a^{25} z^{-2} - 9a^{27} z^{-2} + \\
& + 9a^{29} z^{-2} - 3a^{31} z^{-2} + 3a^9 z^{-1} - 15a^{11} z^{-1} + 21a^{13} z^{-1} + \\
& - 9a^{15} z^{-1} + 4a^{25} - 12a^{27} + 12a^{29} - 4a^{31} + a^9 z - 25a^{11} z + \\
& + 62a^{13} z - 38a^{15} z + 3a^{25} z - 3a^{27} z + a^{25} z^2 - 3a^{27} z^2 + \\
& + 3a^{29} z^2 - a^{31} z^2 - 19a^{11} z^3 + 102a^{13} z^3 - 99a^{15} z^3 + 7a^{25} z^3 + \\
& - 4a^{27} z^3 - 7a^{11} z^5 + 94a^{13} z^5 - 155a^{15} z^5 + 5a^{25} z^5 - a^{27} z^5 + \\
& - a^{11} z^7 + 46a^{13} z^7 - 129a^{15} z^7 + a^{25} z^7 + 11a^{13} z^9 - 56a^{15} z^9 + \\
& + a^{13} z^{11} - 12a^{15} z^{11} - a^{15} z^{13}
\end{aligned}$$

$$\begin{aligned}
J_{4,1}(B_{2,2}) = & a^9 z^{-3} - 3a^{11} z^{-3} + 3a^{13} z^{-3} - a^{15} z^{-3} + 2a^5 z^{-2} - 6a^7 z^{-2} + \\
& + 6a^9 z^{-2} - 2a^{11} z^{-2} + a^{25} z^{-2} - 3a^{27} z^{-2} + 3a^{29} z^{-2} - a^{31} z^{-2} + \\
& + 3a^9 z^{-1} - 15a^{11} z^{-1} + 21a^{13} z^{-1} - 9a^{15} z^{-1} + 2a^5 - 18a^7 + 30a^9 + \\
& - 14a^{11} + 2a^{25} - 6a^{27} + 6a^{29} - 2a^{31} + a^9 z - 25a^{11} z + \\
& + 62a^{13} z - 38a^{15} z + a^{25} z - a^{27} z - 20a^7 z^2 + 70a^9 z^2 + \\
& - 50a^{11} z^2 + a^{25} z^2 - 3a^{27} z^2 + 3a^{29} z^2 - a^{31} z^2 - 19a^{11} z^3 + \\
& + 102a^{13} z^3 - 99a^{15} z^3 + 3a^{25} z^3 - 2a^{27} z^3 - 10a^7 z^4 + 88a^9 z^4 + \\
& - 110a^{11} z^4 - 7a^{11} z^5 + 94a^{13} z^5 - 155a^{15} z^5 + 3a^{25} z^5 - a^{27} z^5 + \\
& - 2a^7 z^6 + 58a^9 z^6 - 128a^{11} z^6 - a^{11} z^7 + 46a^{13} z^7 - 129a^{15} z^7 + \\
& + a^{25} z^7 + 18a^9 z^8 - 74a^{11} z^8 + 11a^{13} z^9 - 56a^{15} z^9 + 2a^9 z^{10} + \\
& - 20a^{11} z^{10} + a^{13} z^{11} - 12a^{15} z^{11} - 2a^{11} z^{12} - a^{15} z^{13}
\end{aligned}$$

## 5 Link Floer Homology in lens spaces

In this section we generalize to the case of links a combinatorial description of the hat version  $\widehat{HFK}$  of the Link Floer Homology developed in [BGH] for knots in lens spaces. Then we compute it on some examples and discuss whether this invariant is essential. We start by recalling some definitions.

**The complex  $(C(G), \partial)$**  Consider a grid diagram  $G = (T^2, \alpha, \beta, \mathbb{O}, \mathbb{X})$  representing an oriented knot in  $L(p, q)$  and denote with  $n$  its grid number. Following [BGH], we associate to  $G$  a chain complex  $(C(G), \partial)$ . Let  $\mathbf{x}$  be an unordered  $n$ -uple of intersection points belonging to  $\alpha \cap \beta$  such that each intersection point belongs to different curves of  $\alpha$  and  $\beta$ . Denote by  $Y$  the set of these elements and let  $C(G)$  be the  $\mathbb{Z}_2$ -module generated by the set  $Y$ . Given  $\mathbf{x} \in Y$ , we call *components* of  $\mathbf{x}$  the points of  $\mathbf{x}$  and we denote by  $x_i$  the only component of  $\mathbf{x}$  laying on the  $\alpha_i$  circle. If  $S_n$  is the symmetric group on  $n$  letters, there is a one to one correspondence between elements of  $Y$  and those of  $S_n \times \mathbb{Z}_p^n$  (see Figure 17). Indeed, an element  $(\sigma, (a_0, \dots, a_{n-1})) \in S_n \times \mathbb{Z}_p^n$  corresponds to the only  $\mathbf{x}$  such that

- $x_i$  lays on  $\alpha_i \cap \beta_{\sigma(i)}$ , for  $i = 0, \dots, n-1$ ;
- $x_i$  is the  $a_i$ -th intersection of  $\alpha_i \cap \beta_{\sigma(i)}$ , for  $i = 0, \dots, n-1$ .

We use the notation  $[c_0, \dots, c_{n-1}]$  to denote the permutation  $\begin{pmatrix} 0 & \dots & n-1 \\ c_0 & \dots & c_{n-1} \end{pmatrix}$ .

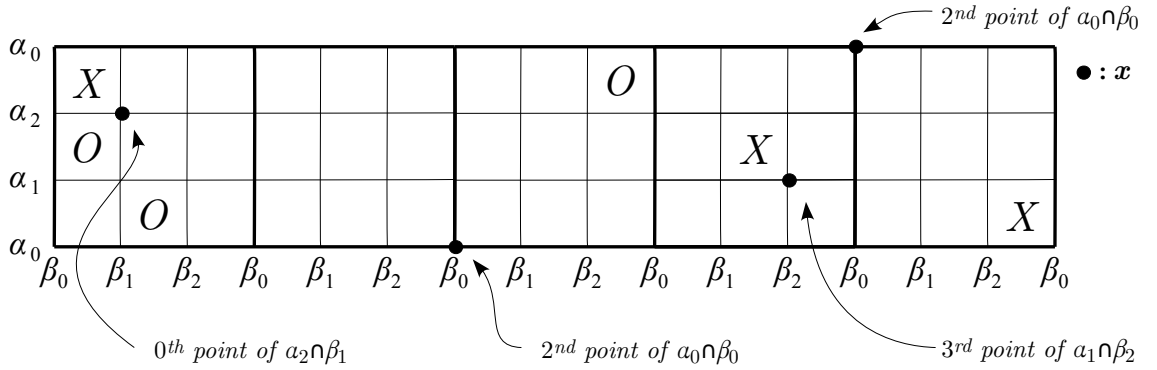


Figure 17: A generator  $\mathbf{x}$  corresponding to  $\{[0 \ 2 \ 1], (2, 3, 0)\} \in S_3 \times \mathbb{Z}_5^3$ .

Now we recall the definition of the boundary operator. A *parallelogram* is a quadrilateral properly embedded in  $T^2$ , that is a quadrilateral having points of  $\alpha \cap \beta$  as vertices and such that its sides coincide with arcs of curves belonging to  $\alpha$  or  $\beta$ . Let  $\mathbf{x}, \mathbf{y} \in Y$  and let  $P$  be a parallelogram; we say that a parallelogram  $P$  *connects*  $\mathbf{x}$  to  $\mathbf{y}$  if

- $\mathbf{x}$  and  $\mathbf{y}$  differ for at most two components  $\{x_i, x_j\}$  and  $\{y_i, y_j\}$  that are vertices of  $P$ ;
- according to the orientation of  $P$  induced by the one fixed on  $T^2$ , the sides of  $P$  belonging to  $\alpha$ 's curves go from  $\mathbf{x}$  vertices to  $\mathbf{y}$  ones.

We call  $R(\mathbf{x}, \mathbf{y})$  the set of parallelograms connecting  $\mathbf{x}$  to  $\mathbf{y}$ . We say that a parallelogram connecting  $\mathbf{x}$  to  $\mathbf{y}$  is *admissible* if its interior contains neither  $\mathbf{x}$  components nor  $\mathbf{y}$  ones. For each pair of generators  $\mathbf{x}, \mathbf{y} \in Y$ , we call  $PG(\mathbf{x}, \mathbf{y})$  the set of admissible parallelograms connecting  $\mathbf{x}$  to  $\mathbf{y}$ . Given a parallelogram  $P$ , denote with  $n_{\mathbb{Q}}(P)$  and  $n_{\mathbb{X}}(P)$ , respectively, the number of



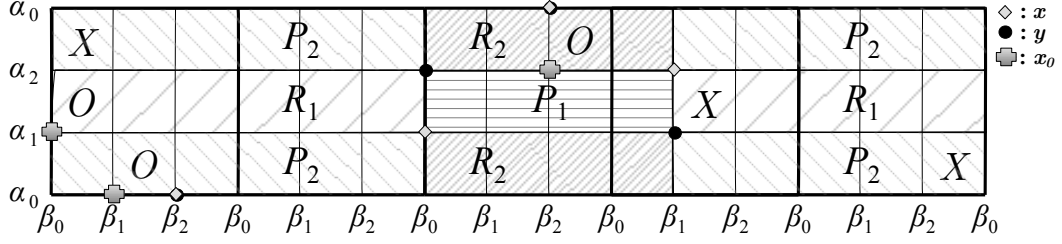


Figure 18: Parallelograms  $P_1$  and  $P_2$  connect  $\mathbf{x}$  to  $\mathbf{y}$ , while  $R_1$  and  $R_2$  connect  $\mathbf{y}$  to  $\mathbf{x}$ . Both  $P_1$  and  $R_1$  are admissible, while  $P_2$  and  $R_2$  are not. Moreover  $n_{\mathbb{O}}(P_1) = n_{\mathbb{X}}(P_1) = 0$ , so the boundary operator connects  $\mathbf{x}$  to  $\mathbf{y}$ .

$O$  markings and  $X$  markings belonging to  $P$  (see Figure 18).

Now we are ready to define a boundary operator  $\partial: C(G) \rightarrow C(G)$

$$\partial \mathbf{x} = \sum_{\mathbf{y} \in Y} \sum_{\left\{ \begin{array}{l} P \in PG(\mathbf{x}, \mathbf{y}) : \\ n_{\mathbb{O}}(P) = n_{\mathbb{X}}(P) = 0 \end{array} \right\}} \mathbf{y}.$$

Since  $\partial^2 = 0$  (see [BGH]), we can define the homology  $H(C(G))$  associated to the chain complex  $(C(G), \partial)$ , obtaining a bigraded  $\mathbb{Z}_2$ -vector space.

**Defining degrees** We can associate to each generator of  $C(G)$  three different degrees: the spin degree, the Maslov degree and the Alexander degree.

Let  $\mathbf{x}_{\mathbb{O}} \in Y$  be the generator whose components are the lower left vertices of the  $n$  distinct parallelograms in  $T^2 - \boldsymbol{\alpha} - \boldsymbol{\beta}$  which contain elements of  $\mathbb{O}$ . Let  $(\sigma_{\mathbb{O}}, (a_0, \dots, a_{n-1}))$  be the element of  $S_n \times \mathbb{Z}_p^n$  corresponding to  $\mathbf{x}_{\mathbb{O}}$  and let  $(\sigma, (b_0, \dots, b_{n-1}))$  be the element corresponding to a generic  $\mathbf{x}$ . The *spin degree* is given by the function  $\mathbf{S}: Y \rightarrow \mathbb{Z}_p$  defined by

$$\mathbf{S}(\mathbf{x}) \equiv [q - 1 + (\sum_{i=0}^{n-1} b_i - \sum_{i=0}^{n-1} a_i)] \mod p. \quad (1)$$

The *Maslov degree* is the function  $\mathbf{M}: Y \rightarrow \mathbb{Q}$  defined by

$$\begin{aligned} \mathbf{M}(\mathbf{x}) = & \frac{1}{p}(I(\widetilde{W}(\mathbf{x}), \widetilde{W}(\mathbf{x})) - I(\widetilde{W}(\mathbf{x}), \widetilde{W}(\mathbb{O})) - I(\widetilde{W}(\mathbb{O}), \widetilde{W}(\mathbf{x})) + \\ & + I(\widetilde{W}(\mathbb{O}), \widetilde{W}(\mathbb{O})) + 1) + d(p, q, q-1) + \frac{p-1}{p}, \end{aligned} \quad (2)$$

where  $d$  is a kind of normalization function depending only on lens space parameters, while  $I$  and  $\widetilde{W}$  are two functions depending on the arrangement of the  $\mathbf{x}$  points with respect to the  $\mathbb{O}$  points (for details see the Appendix).

Finally, the *Alexander degree* is a function  $\mathbf{A}: Y \rightarrow \mathbb{Q}$  defined by

$$\mathbf{A}(\mathbf{x}) = \frac{1}{2}(\mathbf{M}_{\mathbb{O}}(\mathbf{x}) - \mathbf{M}_{\mathbb{X}}(\mathbf{x}) - (n-1)), \quad (3)$$

where  $\mathbf{M}_{\mathbb{O}}$  is the Maslov degree and  $\mathbf{M}_{\mathbb{X}}$  is the degree obtained by replacing  $\mathbb{O}$  with  $\mathbb{X}$  in formula (2).

The following equations show how the boundary operator relate with these degrees

$$\mathbf{S}(\partial(\mathbf{x})) = \mathbf{S}(\mathbf{x}) \quad \mathbf{M}(\partial(\mathbf{x})) = \mathbf{M}(\mathbf{x}) - 1 \quad \mathbf{A}(\partial(\mathbf{x})) = \mathbf{A}(\mathbf{x}). \quad (4)$$

**Knot Floer Homology** Let  $V$  be a bidimensional  $\mathbb{Z}_2$ -vector space spanned by a vector with Maslov-Alexander bigrading  $(-1, -1)$  and another one with Maslov-Alexander bigrading  $(0, 0)$ .

**Proposition 10** ([BGH, MOS]). *Consider a grid diagram  $G_K$  of an oriented knot  $K \subset L(p, q)$ . Then  $H(C(G_K), \partial)$  is isomorphic to the bigraded group  $\widehat{HFK}(K) \otimes V^{\otimes(n-1)}$ , where  $n$  is the grid number of  $G$ .*

**Link Floer Homology** In this paragraph we generalize the combinatorial computation of  $\widehat{HFL}$  to the case of links. Let  $L \subset L(p, q)$  be an oriented link with  $l$  components  $L_1, \dots, L_l$  and let  $G_L = (T^2, \boldsymbol{\alpha}, \boldsymbol{\beta}, \mathbb{O}, \mathbb{X})$  be a grid diagram of it. Let  $k_j$  be the number of  $\mathbb{O}$  markings belonging to  $L_j$  (which is equal to the one of  $\mathbb{X}$  markings) and denote elements of  $\mathbb{O}$  or  $\mathbb{X}$  belonging to  $L_j$  with as  $O_{j,i}$  or  $X_{j,i}$  for  $j = 1, \dots, l$  and  $i = 1, \dots, k_j$ . The generators of  $C(G_L)$ ,

the boundary operator, the spin degree and the Maslov degree are defined as in the case of knots. Instead, the Alexander degree becomes a multidegree as follows. Consider the set  $\mathbb{O}_j$  composed by elements of  $\mathbb{O}$  belonging to  $L_j$ . Let  $\mathbf{M}_{\mathbb{O}_j}(\mathbf{x})$  be the Maslov degree of  $\mathbf{x}$ , computed with respect to  $\mathbb{O}_j$ . The Alexander multidegree is the function  $\mathbf{A}: Y \rightarrow \mathbb{Q}^l$  defined by

$$\mathbf{A}(\mathbf{x}) = \frac{1}{2} \left( \mathbf{M}_{\mathbb{O}_1}(\mathbf{x}) - \mathbf{M}_{\mathbb{X}_1}(\mathbf{x}) - (n_1 - 1), \dots, \mathbf{M}_{\mathbb{O}_l}(\mathbf{x}) - \mathbf{M}_{\mathbb{X}_l}(\mathbf{x}) - (n_l - 1) \right).$$

As in the case of knots, we can define the homology  $H(C(G_L), \partial)$  of the chain complex  $(C(G_L), \partial)$ . For  $j = 1, \dots, l$ , let  $V_j$  be a bidimensional  $\mathbb{Z}_2$ -vector space, spanned by a vector with Maslov-Alexander multidegree  $(0, (0, 0, \dots, 0))$  and another one with multidegree  $(-1, -\vec{e}_j)$ , where  $\vec{e}_j$  indicates the  $j$ -th vector of the canonical basis of  $\mathbb{R}^l$ .

**Proposition 11.** *Let  $L$  be an oriented link in  $L(p, q)$ , and let  $G_L$  be a grid diagram of  $L$ . Denote with  $L_1, \dots, L_l$  the components of  $L$ . Then*

$$H(C(G_L), \partial) \cong \widehat{HFL}(L) \otimes \bigotimes_{j=1}^l V_j^{\otimes (k_j - 1)},$$

where  $k_j$  is the number of  $O$  markings belonging to  $L_j$ .

*Proof.* Since Proposition 7.2 of [OS] holds also in the case of lens spaces, by using an argument similar to the one used in proof of Proposition 2.5 of [MOS], we can conclude.  $\square$

**Behavior under change of orientation** Let  $G_K$  be a grid diagram of an oriented knot  $K \subset L(p, q)$  and let  $-G_K$  be a grid diagram of  $-K$ , obtained exchanging the elements of  $\mathbb{O}$  and  $\mathbb{X}$  in  $G_K$ .

**Proposition 12.** *There is a one to one correspondence between the generators of  $H(C(G_K), \partial)$  and those of  $H(C(-G_K), \partial)$ : a generator of  $H(C(G_K), \partial)$  having spin degree  $s$ , Maslov degree  $m$  and Alexander degree  $a$  corresponds to a generator of  $H(C(-G_K), \partial)$  with spin degree  $s + k$ , Maslov degree  $m - 2a - (n - 1)$  and Alexander degree  $-a - (n - 1)$ , where  $k$  is a fixed integer and  $n$  denote the grid number of  $G_K$ .*

*Proof.* Clearly the generators of  $C(G_K)$  coincide with those of  $C(-G_K)$ , but for simplicity's sake, given  $\mathbf{x} \in C(G_K)$  we denote with  $-\mathbf{x}$  the same generator thought in  $C(-G_K)$ . Moreover, two generators  $\mathbf{x}, \mathbf{y} \in (C(G_K), \partial)$  are connected by the boundary operator if and only if  $-\mathbf{x}$  and  $-\mathbf{y}$  are connected by the boundary operator in the chain complex  $(C(-G_K), \partial)$ . Thus generators of  $H(C(G_K), \partial)$  coincide with those of  $H(C(-G_K), \partial)$ . On the contrary,  $\mathbf{x}$  and  $-\mathbf{x}$  have generally different degrees. By definition we have

$$\mathbf{M}(-x) = \mathbf{M}_{\mathbb{O}}(-\mathbf{x}) = \mathbf{M}_{\mathbb{X}}(\mathbf{x}) = \mathbf{M}_{\mathbb{O}}(\mathbf{x}) - 2A(\mathbf{x}) - (n-1)$$

and

$$\begin{aligned} \mathbf{A}(-\mathbf{x}) &= \frac{1}{2}(\mathbf{M}_{\mathbb{O}}(-\mathbf{x}) - \mathbf{M}_{\mathbb{X}}(-\mathbf{x}) - (n-1)) = \frac{1}{2}(\mathbf{M}_{\mathbb{X}}(\mathbf{x}) - \mathbf{M}_{\mathbb{O}}(\mathbf{x}) - (n-1)) = \\ &= \frac{1}{2}(\mathbf{M}_{\mathbb{O}}(\mathbf{x}) - 2\mathbf{A}(\mathbf{x}) - (n-1) - \mathbf{M}_{\mathbb{O}}(\mathbf{x}) - (n-1)) = -\mathbf{A}(\mathbf{x}) - (n-1). \end{aligned}$$

Let  $\mathbf{x}_{\mathbb{O}} = \{\sigma_{\mathbb{O}}, (b_0, \dots, b_{n-1})\}$  (resp.  $\mathbf{x}_{\mathbb{X}} = \{\sigma_{\mathbb{X}}, (c_0, \dots, c_{n-1})\}$ ) be the generators of  $C(G_K)$  whose components are lower left vertices of the  $n$  distinct parallelograms in  $T^2 - \alpha - \beta$  containing elements of  $\mathbb{O}$  (resp.  $\mathbb{X}$ ). Set  $k := \sum_{i=0}^{n-1} b_i - \sum_{i=0}^{n-1} c_i \pmod{p}$ . Then we have

$$\mathbf{S}(-\mathbf{x}) = \mathbf{S}(\mathbf{x}) + k.$$

□

Observe that, according to Proposition 11, if  $G_K$  has grid number 1, then  $\widehat{HFK}(K) = H(C(G_K), \partial)$ , as a consequence  $\widehat{HFK}(-K)$  can be achieved straightly from  $\widehat{HFK}(K)$ .

**Example 13.** In the Appendix, we compute the Knot Floer Homology of both the knots  $K_1$  and  $-K_1$  depicted in Figure 14, using a grid diagram with grid number 1. We obtain

$$\begin{aligned} \widehat{HFK}(K_1) &\cong \mathbb{Z}_2[0, -\frac{2}{5}, -\frac{1}{5}] \oplus \mathbb{Z}_2[1, -\frac{2}{5}, -\frac{2}{5}] \oplus \mathbb{Z}_2[2, \frac{2}{5}, \frac{2}{5}] \oplus \mathbb{Z}_2[3, 0, \frac{1}{5}] \oplus \\ &\oplus \mathbb{Z}_2[4, \frac{2}{5}, 0] \end{aligned}$$

and

$$\widehat{HFK}(-K_1) \cong \mathbb{Z}_2[2, 0, \frac{1}{5}] \oplus \mathbb{Z}_2[3, \frac{2}{5}, \frac{2}{5}] \oplus \mathbb{Z}_2[4, -\frac{2}{5}, -\frac{2}{5}] \oplus \mathbb{Z}_2[0, -\frac{2}{5}, -\frac{1}{5}] \oplus \mathbb{Z}_2[1, \frac{2}{5}, 0]$$

where  $\mathbb{Z}_2[i, j, k]$  denotes a  $\mathbb{Z}_2$ -vector space spanned by a generator with spin degree  $i$ , Maslov degree  $j$  and Alexander degree  $k$ . This value of  $\widehat{HFK}(-K_1)$  clearly coincides with the one obtained using Proposition 12 (with  $k = 2$ ).

To end this section we compute  $\widehat{HFL}$  on the pairs of links of Examples 7 and 8 in order to test whereas this invariant is essential or not. Computations are very long so we report them in the Appendix, while here we collect only the results, showing that  $\widehat{HFL}$  can distinguish both the pairs of links.

**Example 14.** Let  $K_1$  and  $K_2$  be the two non equivalent knots in  $L(5, 2)$ , depicted in Figure 14, both lifting to the trivial knots in  $\mathbf{S}^3$  (see [Ma1]). We have

$$\widehat{HFK}(K_1) \cong \mathbb{Z}_2[0, -\frac{2}{5}, -\frac{1}{5}] \oplus \mathbb{Z}_2[1, -\frac{2}{5}, -\frac{2}{5}] \oplus \mathbb{Z}_2[2, \frac{2}{5}, \frac{2}{5}] \oplus \mathbb{Z}_2[3, 0, \frac{1}{5}] \oplus \mathbb{Z}_2[4, \frac{2}{5}, 0]$$

and

$$\widehat{HFK}(K_2) \cong \mathbb{Z}_2[0, -\frac{2}{5}, 0] \oplus \mathbb{Z}_2[1, -\frac{2}{5}, -\frac{2}{5}] \oplus \mathbb{Z}_2[2, \frac{2}{5}, \frac{1}{5}] \oplus \mathbb{Z}_2[3, 0, -\frac{1}{5}] \oplus \mathbb{Z}_2[4, \frac{2}{5}, \frac{2}{5}].$$

**Example 15.** Let  $L_A$  and  $L_B$  be the two non equivalent links in  $L(4, 1)$ , depicted in Figure 15 both lifting to the Hopf link in  $\mathbf{S}^3$  (see [Ma1]). We have

$$\widehat{HFL}(L_A) \cong \mathbb{Z}_2[0, \frac{1}{2}, \frac{1}{2}] \oplus \mathbb{Z}_2[1, \frac{1}{2}, -\frac{1}{2}] \oplus \mathbb{Z}_2[2, -\frac{1}{2}, \frac{1}{2}] \oplus \mathbb{Z}_2[3, -\frac{1}{2}, -\frac{1}{2}]$$

and

$$\begin{aligned}
\widehat{HFL}(L_B) \cong H(C(G_B), \partial) \cong & \mathbb{Z}_2 \left[ 0, \frac{1}{4}, \left( \frac{1}{8}, \frac{1}{8} \right) \right] \oplus \mathbb{Z}_2 \left[ 0, -\frac{3}{4}, \left( -\frac{7}{8}, \frac{1}{8} \right) \right] \oplus \\
& \oplus \mathbb{Z}_2 \left[ 0, -\frac{3}{4}, \left( \frac{1}{8}, -\frac{7}{8} \right) \right] \oplus \mathbb{Z}_2 \left[ 0, -\frac{7}{4}, \left( -\frac{7}{8}, -\frac{7}{8} \right) \right] \oplus \mathbb{Z}_2 \left[ 1, 0, \left( -\frac{5}{8}, -\frac{1}{8} \right) \right] \oplus \\
& \oplus \mathbb{Z}_2 \left[ 1, -1, \left( -\frac{5}{8}, -\frac{1}{8} \right) \right] \oplus \mathbb{Z}_2 \left[ 2, \frac{1}{4}, \left( -\frac{3}{8}, -\frac{3}{8} \right) \right] \oplus \mathbb{Z}_2 \left[ 2, -\frac{3}{4}, \left( -\frac{3}{8}, -\frac{3}{8} \right) \right]^3 \oplus \\
& \oplus \mathbb{Z}_2 \left[ 3, 0, \left( -\frac{1}{8}, -\frac{5}{8} \right) \right] \oplus \mathbb{Z}_2 \left[ 3, -1, \left( -\frac{1}{8}, -\frac{5}{8} \right) \right]
\end{aligned}$$

where  $\mathbb{Z}_2[i, j, (k_1, k_2)]$  denotes a  $\mathbb{Z}_2$ -vector spanned by a generator with spin degree  $i$ , Maslov degree  $j$  and Alexander bigrading  $(k_1, k_2)$ .

## 6 Appendix

This appendix contains the computations of Examples 14 and 15.

**Maslov index** First of all we recall the definition of the functions  $d, I$  and  $\widetilde{W}$  appearing in the formula (2) of the Maslov index (see [BGH] for details). In order to compute these functions it is more easy to keep slanted grid diagrams.

Let  $G = (T^2, \boldsymbol{\alpha}, \boldsymbol{\beta}, \mathbb{O}, \mathbb{X})$  be a grid diagram representing a link in  $L(p, q)$  and let  $n$  be its grid number. We denote with  $d: \mathbb{Z} \times \mathbb{Z} \times \mathbb{Z} \rightarrow \mathbb{Q}$  be the function defined by induction as

$$\begin{aligned}
d(1, 0, 0) &= 0 \\
d(p, q, i) &= \left( \frac{pq - (2i + 1 - p - q)^2}{4pq} \right) - d(q, r, j)
\end{aligned}$$

where  $r \equiv p \pmod{q}$  and  $j \equiv i \pmod{q}$ . Consider the function

$$W: \left\{ \begin{array}{l} \text{Finite set of} \\ \text{points in } G \end{array} \right\} \rightarrow \left\{ \begin{array}{l} \text{Finite set of pairs } (a, b) \\ \text{with } a \in [0, pn), b \in [0, n) \end{array} \right\}$$

that associates to a  $n$ -ple of points of  $G$  their coordinates in  $\mathbb{R}^2$  with respect to the base

$$\left( \vec{v}_1 = \left( \frac{1}{np}, 0 \right), \vec{v}_2 = \left( -\frac{q}{np}, \frac{1}{n} \right) \right).$$

Assume that the points of  $\mathbb{O}$  and  $\mathbb{X}$  are placed in the centre of their respective parallelograms. In this way, with respect to the basis  $(\vec{v}_1, \vec{v}_2)$ , the generators  $\mathbf{x}$  have integer coordinates, whereas the points of  $\mathbb{O}$  and  $\mathbb{X}$  have rational coordinates. Now define the function

$$C_{p,q}: \left\{ \begin{array}{l} \text{Finite sets of pairs (a,b)} \\ \text{where } a \in [0, pn), b \in [0, n) \end{array} \right\} \rightarrow \left\{ \begin{array}{l} \text{Finite sets of pairs (a,b)} \\ \text{where } a, b \in [0, pn) \end{array} \right\}$$

that, to a  $n$ -uple of coordinates

$$((a_i, b_i))_{i=0}^{n-1}$$

associates a  $pn$ -uple of coordinates

$$(a_i + nqk \mod np, b_i + nk)_{i=0, k=0}^{i=n-1, k=p-1}.$$

Let  $A$  and  $B$  be two finite sets of pairs of coordinates and  $I$  be the function that, to a ordinate pair  $(A, B)$ , associates the cardinality of the set of the pairs  $(a, b) \in A \times B$ ,  $a = (a_1, a_2) \in A$ ,  $b = (b_1, b_2) \in B$ , such that  $a_i < b_i$  for  $i = 1, 2$ . Define  $\widetilde{W} := C_{p,q} \circ W$ .

**Computation of examples 13 and 14** To compute the Link Floer Homology of the oriented knots  $K_1, K_2 \subset L(5, 2)$  depicted in Figure 14, we use the slanted grid diagrams  $G_1$  and  $G_2$  depicted in Figure 19. Both the of generators of both  $C(G_1)$  and  $C(G_2)$  are in one to one correspondence with  $S_1 \times \mathbb{Z}_5$  and hence they consist of five elements that we denote with  $\{\{[0], (0)\}, \{[0], (1)\}, \{[0], (2)\}, \{[0], (3)\}, \{[0], (4)\}\}$ .

Let us compute the spin degree of each generator. First, observe that for both  $G_1$  and  $G_2$ , we have that  $\{[0], (0)\} = x_{\mathbb{O}}$ . So, from formula (1), we get

$$\mathbf{S}(\{[0], (i)\}) \equiv [2 - 1 + (i - 0)] \equiv 0 \mod 5, \forall i = 0, \dots, 4.$$

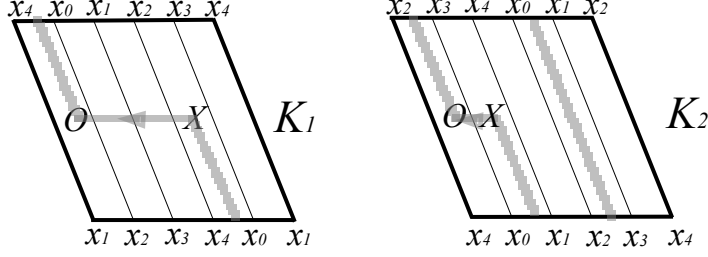


Figure 19: Grid diagrams  $G_1$  and  $G_2$ .

Then, if  $x_i$  denotes the generator having spin degree  $i$ , we have

$$x_0 := \{[0], (4)\}, \quad x_1 := \{[0], (0)\}, \quad x_2 := \{[0], (1)\}, \quad x_3 := \{[0], (2)\}, \quad x_4 := \{[0], (3)\}.$$

Now we deal with the Maslov degree starting by computing the values assumed by the function  $d$

$$\begin{aligned} d(p, q, q-1) &= d(5, 2, 1) = \left( \frac{10 - (2 + 1 - 5 - 2)^2}{4 \cdot 5 \cdot 2} \right) - d(2, 1, 1) = \\ &= -\frac{6}{40} - d(2, 1, 1) = -\frac{3}{20} - \left( \frac{2 - (2 + 1 - 2 - 1)^2}{4 \cdot 2 \cdot 1} \right) - d(1, 0, 0) = \\ &= -\frac{3}{20} - \frac{1}{4} - 0 = -\frac{2}{5}. \end{aligned}$$

Denote with  $Z$  the  $X$  marking of  $G_2$ . The elements  $x_i, O, X$  and  $Z$ , considered as points of the unitary square  $[0, 1] \times [0, 1]$ , have the following coordinates with respect to the canonical basis

$$\begin{aligned} x_0 &= \left( \frac{4}{5}, 0 \right) & x_1 &= (0, 0) & x_2 &= \left( \frac{1}{5}, 0 \right) & x_3 &= \left( \frac{2}{5}, 0 \right) & x_4 &= \left( \frac{3}{5}, 0 \right) \\ O &= \left( \frac{9}{10}, \frac{1}{2} \right) & X &= \left( \frac{1}{2}, \frac{1}{2} \right) & Z &= \left( \frac{1}{10}, \frac{1}{2} \right). \end{aligned}$$

The grid diagrams  $G_1$  and  $G_2$  have grid number  $n = 1$ , so, switching to the basis  $\left( \vec{v}_1 = \left( \frac{1}{np}, 0 \right) = \left( \frac{1}{5}, 0 \right), \vec{v}_2 = \left( -\frac{q}{np}, \frac{1}{n} \right) = \left( -\frac{2}{5}, 1 \right) \right)$  by means of



the basis change matrix  $W = \begin{pmatrix} np & nq \\ 0 & n \end{pmatrix} = \begin{pmatrix} 5 & 2 \\ 0 & 1 \end{pmatrix}$ , we get the following values.

	$x_0$	$x_1$	$x_2$	$x_3$	$x_4$	$O$	$X$	$Z$
W(column)	$(4, 0)$	$(0, 0)$	$(1, 0)$	$(2, 0)$	$(3, 0)$	$\left(\frac{11}{2}, \frac{1}{2}\right)$	$\left(\frac{7}{2}, \frac{1}{2}\right)$	$\left(\frac{3}{2}, \frac{1}{2}\right)$

By composing with the function  $C_{5,2}$  we have

$$\begin{aligned}
\widetilde{W}(x_0) &= ((4 \bmod 5, 0), (1 \bmod 5, 1), (3 \bmod 5, 2), (0 \bmod 5, 3), (2 \bmod 5, 4)) \\
\widetilde{W}(x_1) &= ((0 \bmod 5, 0), (2 \bmod 5, 1), (4 \bmod 5, 2), (1 \bmod 5, 3), (3 \bmod 5, 4)) \\
\widetilde{W}(x_2) &= ((1 \bmod 5, 0), (3 \bmod 5, 1), (0 \bmod 5, 2), (2 \bmod 5, 3), (4 \bmod 5, 4)) \\
\widetilde{W}(x_3) &= ((2 \bmod 5, 0), (4 \bmod 5, 1), (1 \bmod 5, 2), (3 \bmod 5, 3), (0 \bmod 5, 4)) \\
\widetilde{W}(x_4) &= ((3 \bmod 5, 0), (0 \bmod 5, 1), (2 \bmod 5, 2), (4 \bmod 5, 3), (1 \bmod 5, 4)) \\
\widetilde{W}(O) &= \left( \left( \frac{1}{2} \bmod 5, \frac{1}{2} \right), \left( \frac{5}{2} \bmod 5, \frac{3}{2} \right), \left( \frac{9}{2} \bmod 5, \frac{5}{2} \right), \left( \frac{3}{2} \bmod 5, \frac{7}{2} \right), \left( \frac{7}{2} \bmod 5, \frac{9}{2} \right) \right) \\
\widetilde{W}(X) &= \left( \left( \frac{7}{2} \bmod 5, \frac{1}{2} \right), \left( \frac{1}{2} \bmod 5, \frac{3}{2} \right), \left( \frac{5}{2} \bmod 5, \frac{5}{2} \right), \left( \frac{9}{2} \bmod 5, \frac{7}{2} \right), \left( \frac{3}{2} \bmod 5, \frac{9}{2} \right) \right) \\
\widetilde{W}(Z) &= \left( \left( \frac{3}{2} \bmod 5, \frac{1}{2} \right), \left( \frac{7}{2} \bmod 5, \frac{3}{2} \right), \left( \frac{1}{2} \bmod 5, \frac{5}{2} \right), \left( \frac{5}{2} \bmod 5, \frac{7}{2} \right), \left( \frac{9}{2} \bmod 5, \frac{9}{2} \right) \right)
\end{aligned}$$

and so we obtain

$J(row, column)$	$x_0$	$x_1$	$x_2$	$x_3$	$x_4$	$O$	$X$	$Z$
$x_0$	3					10	7	8
$x_1$		7				12	8	8
$x_2$			7			10	10	9
$x_3$				3		9	8	6
$x_4$					5	9	7	9
$O$	5	7	5	4	4	7		
$X$	2	3	5	3	2		3	
$Z$	3	3	4	1	4			3

where with  $J(Y_1, Y_2)$  we denote the function  $I(\widetilde{W}(Y_1), \widetilde{W}(Y_2))$ . Finally, from

formula (2) we get

$$\begin{aligned}
\mathbf{M}(x_0) &= \mathbf{M}_{\mathbb{O}}(x_0) = \frac{1}{5}(3 - 10 - 5 + 7 + 1) - \frac{2}{5} + \frac{4}{5} = -\frac{2}{5} \\
\mathbf{M}(x_1) &= \mathbf{M}_{\mathbb{O}}(x_1) = \frac{1}{5}(7 - 12 - 7 + 7 + 1) - \frac{2}{5} + \frac{4}{5} = -\frac{2}{5} \\
\mathbf{M}(x_2) &= \mathbf{M}_{\mathbb{O}}(x_2) = \frac{1}{5}(7 - 10 - 5 + 7 + 1) - \frac{2}{5} + \frac{4}{5} = \frac{2}{5} \\
\mathbf{M}(x_3) &= \mathbf{M}_{\mathbb{O}}(x_3) = \frac{1}{5}(3 - 9 - 4 + 7 + 1) - \frac{2}{5} + \frac{4}{5} = 0 \\
\mathbf{M}(x_4) &= \mathbf{M}_{\mathbb{O}}(x_4) = \frac{1}{5}(5 - 9 - 4 + 7 + 1) - \frac{2}{5} + \frac{4}{5} = \frac{2}{5}.
\end{aligned}$$

Observe that, since  $O$  lies in the same cell for both  $G_1$  and  $G_2$ , the Maslov degree is the same for generators of  $C(G_1)$  and  $C(G_2)$ .

Similarly, we compute the Maslov degree with respect to  $\mathbb{X}$  and to  $\mathbb{Z}$  obtaining

$$\begin{aligned}
\mathbf{M}_{\mathbb{X}}(x_0) &= \frac{1}{5}(3 - 7 - 2 + 3 + 1) - \frac{2}{5} + \frac{4}{5} = 0 \\
\mathbf{M}_{\mathbb{X}}(x_1) &= \frac{1}{5}(7 - 8 - 3 + 3 + 1) - \frac{2}{5} + \frac{4}{5} = \frac{2}{5} \\
\mathbf{M}_{\mathbb{X}}(x_2) &= \frac{1}{5}(7 - 10 - 5 + 3 + 1) - \frac{2}{5} + \frac{4}{5} = -\frac{2}{5} \\
\mathbf{M}_{\mathbb{X}}(x_3) &= \frac{1}{5}(3 - 8 - 3 + 3 + 1) - \frac{2}{5} + \frac{4}{5} = -\frac{2}{5} \\
\mathbf{M}_{\mathbb{X}}(x_4) &= \frac{1}{5}(5 - 7 - 2 + 3 + 1) - \frac{2}{5} + \frac{4}{5} = \frac{2}{5} \\
\mathbf{M}_{\mathbb{Z}}(x_0) &= \frac{1}{5}(3 - 8 - 3 + 3 + 1) - \frac{2}{5} + \frac{4}{5} = -\frac{2}{5} \\
\mathbf{M}_{\mathbb{Z}}(x_1) &= \frac{1}{5}(7 - 8 - 3 + 3 + 1) - \frac{2}{5} + \frac{4}{5} = \frac{2}{5} \\
\mathbf{M}_{\mathbb{Z}}(x_2) &= \frac{1}{5}(7 - 9 - 4 + 3 + 1) - \frac{2}{5} + \frac{4}{5} = 0 \\
\mathbf{M}_{\mathbb{Z}}(x_3) &= \frac{1}{5}(3 - 6 - 1 + 3 + 1) - \frac{2}{5} + \frac{4}{5} = \frac{2}{5} \\
\mathbf{M}_{\mathbb{Z}}(x_4) &= \frac{1}{5}(5 - 9 - 4 + 3 + 1) - \frac{2}{5} + \frac{4}{5} = -\frac{2}{5}.
\end{aligned}$$

Now, using formula (3), we can compute, on one hand, the Alexander

degree of  $C(G_1)$  generators

$$\begin{aligned}
\mathbf{A}(x_0) &= \frac{1}{2}(\mathbf{M}_{\mathbb{O}}(x_0) - \mathbf{M}_{\mathbb{X}}(x_0) - (n-1)) = \frac{1}{2}(-\frac{2}{5} - 0 - 0) = -\frac{1}{5} \\
\mathbf{A}(x_1) &= \frac{1}{2}(-\frac{2}{5} - \frac{2}{5}) = -\frac{2}{5} \\
\mathbf{A}(x_2) &= \frac{1}{2}(\frac{2}{5} + \frac{2}{5}) = \frac{2}{5} \\
\mathbf{A}(x_3) &= \frac{1}{2}(0 + \frac{2}{5}) = \frac{1}{5} \\
\mathbf{A}(x_4) &= \frac{1}{2}(\frac{2}{5} - \frac{2}{5}) = 0,
\end{aligned}$$

and, on the other hand, the Alexander degree of  $C(G_2)$  generators

$$\begin{aligned}
\mathbf{A}(x_0) &= \frac{1}{2}(-\frac{2}{5} + \frac{2}{5} - 0) = 0 \\
\mathbf{A}(x_1) &= \frac{1}{2}(-\frac{2}{5} - \frac{2}{5}) = -\frac{2}{5} \\
\mathbf{A}(x_2) &= \frac{1}{2}(\frac{2}{5} + 0) = \frac{1}{5} \\
\mathbf{A}(x_3) &= \frac{1}{2}(0 - \frac{2}{5}) = -\frac{1}{5} \\
\mathbf{A}(x_4) &= \frac{1}{2}(\frac{2}{5} + \frac{2}{5}) = \frac{2}{5}.
\end{aligned}$$

In the following tables we resume the Maslov and Alexander degrees of the generators.

$C(G_1)$	$x_0$	$x_1$	$x_2$	$x_3$	$x_4$
<b>M</b>	$-\frac{2}{5}$	$-\frac{2}{5}$	$\frac{2}{5}$	0	$\frac{2}{5}$
<b>A</b>	$-\frac{1}{5}$	$-\frac{2}{5}$	$\frac{2}{5}$	$\frac{1}{5}$	0

$C(G_2)$	$x_0$	$x_1$	$x_2$	$x_3$	$x_4$
<b>M</b>	$-\frac{2}{5}$	$-\frac{2}{5}$	$\frac{2}{5}$	0	$\frac{2}{5}$
<b>A</b>	0	$-\frac{2}{5}$	$\frac{1}{5}$	$-\frac{1}{5}$	$\frac{2}{5}$

After computing the three degrees for each generator, we look for pairs of generators connected by the boundary operator. Since the generators of  $C(G_1)$  have different spin degree and, by formula (4), the boundary operator  $\partial$  preserves the spin degree, there is no connection via boundary operator between the five generators. This means that each generator of  $C(G_1)$  is a generator of  $H(C(G_1), \partial)$ . Hence, by Proposition 10, we get

$$\widehat{HFK}(K_1) \cong H(C(G_1), \partial) \cong \mathbb{Z}_2[0, -\frac{2}{5}, -\frac{1}{5}] \oplus \mathbb{Z}_2[1, -\frac{2}{5}, -\frac{2}{5}] \oplus \mathbb{Z}_2[2, \frac{2}{5}, \frac{2}{5}] \oplus \mathbb{Z}_2[3, 0, \frac{1}{5}] \oplus \mathbb{Z}_2[4, \frac{2}{5}, 0],$$

where  $\mathbb{Z}_2[i, j, k]$  denotes a  $\mathbb{Z}_2$ -vector space embedded with spin degree  $i$ , Maslov degree  $j$  and Alexander degree  $k$ .

Similarly we get

$$\widehat{HFK}(K_1) \cong H(C(G_2), \partial) \cong \mathbb{Z}_2[0, -\frac{2}{5}, 0] \oplus \mathbb{Z}_2[1, -\frac{2}{5}, -\frac{2}{5}] \oplus \mathbb{Z}_2[2, \frac{2}{5}, \frac{1}{5}] \oplus \mathbb{Z}_2[3, 0, -\frac{1}{5}] \oplus \mathbb{Z}_2[4, \frac{2}{5}, \frac{2}{5}].$$

By a straightforward computation we obtain

$$\widehat{HFK}(-K_1) \cong \mathbb{Z}_2[0, -\frac{2}{5}, -\frac{1}{5}] \oplus \mathbb{Z}_2[1, \frac{2}{5}, 0] \oplus \mathbb{Z}_2[2, 0, \frac{1}{5}] \oplus \mathbb{Z}_2[3, \frac{2}{5}, \frac{2}{5}] \oplus \mathbb{Z}_2[4, -\frac{2}{5}, -\frac{2}{5}],$$

as predicted by Proposition 12.

**Computation of example 14** We compute the Link Floer Homology of the links  $L_A, L_B \subset L(4, 1)$  of Figure 15. Using the grid diagram with grid number one depicted in the figure, the computations for the knot  $L_A$  are really similar to the ones done in the previous example. We get

$$\widehat{HFL}(L_A) \cong \mathbb{Z}_2[0, \frac{1}{2}, \frac{1}{2}] \oplus \mathbb{Z}_2[1, \frac{1}{2}, -\frac{1}{2}] \oplus \mathbb{Z}_2[2, -\frac{1}{2}, \frac{1}{2}] \oplus \mathbb{Z}_2[3, -\frac{1}{2}, -\frac{1}{2}].$$

Much more work is necessary to compute the Link Floer Homology of the two components link  $L_B$ . Referring to Figure 20, we identify the set of the generators of  $C(G_B)$  with the set composed by pairs  $x_i y_j$  and by pairs  $x'_i y'_j$  for  $i, j \in \{1, \dots, p\}$ . By formula (1), we get

$$\mathbf{S}(x_i y_j) \equiv i + j \equiv \mathbf{S}(x'_i y'_j) \pmod{p}.$$

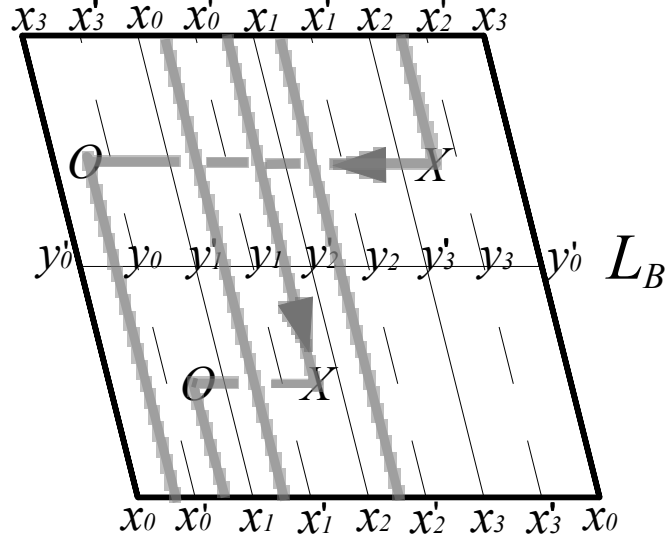


Figure 20: Grid diagram  $G_B$  for the link  $L_B \subset L(4, 1)$ .

Implementing the algorithm described in the first paragraph of the Appendix, we can use a calculator to compute both the Maslov and the Alexander degrees of the generators of  $C(G_B)$ . The results are contained in the four tables starting at page 36.

Once we have computed all the three degrees, we want to establish which generators are connected by the boundary operator. From formula (4), two generators of  $C(G_B)$ , may be connected by the boundary operator if they have the same spin and Alexander degrees and if their Maslov degrees differ by 1. Given two such generators  $\mathbf{x}$  and  $\mathbf{y}$ , consider the set  $N_{\mathbf{x}, \mathbf{y}}$  of admissible parallelograms connecting them and containing neither  $O$  nor  $X$ . We have that the boundary operator connects  $\mathbf{x}$  and  $\mathbf{y}$  if and only if  $\#(N_{\mathbf{x}, \mathbf{y}}) \equiv 1 \pmod 2$ .

	<b>A<sub>0</sub></b>	<b>B<sub>0</sub></b>	<b>C<sub>0</sub></b>	<b>D<sub>0</sub></b>	<b>E<sub>0</sub></b>	<b>F<sub>0</sub></b>	<b>G<sub>0</sub></b>	<b>H<sub>0</sub></b>
<b>S</b> = 0	$x_0 y_0$	$x'_0 y'_0$	$x_1 y_3$	$x'_1 y'_3$	$x_2 y_2$	$x'_2 y'_2$	$x_3 y_1$	$x'_3 y'_1$
<b>M</b>	$-\frac{3}{4}$	$-\frac{7}{4}$	$-\frac{3}{4}$	$\frac{1}{4}$	$\frac{5}{4}$	$\frac{1}{4}$	$-\frac{3}{4}$	$-\frac{7}{4}$
<b>A</b>	$(-\frac{7}{8}, -\frac{7}{8})$	$(-\frac{7}{8}, -\frac{7}{8})$	$(-\frac{7}{8}, \frac{1}{8})$	$(\frac{1}{8}, \frac{1}{8})$	$(\frac{1}{8}, \frac{1}{8})$	$(\frac{1}{8}, \frac{1}{8})$	$(\frac{1}{8}, -\frac{7}{8})$	$(-\frac{7}{8}, -\frac{7}{8})$

Table 1: Generators of  $C(G_B)$  having spin degree 0.

	<b>A<sub>1</sub></b>	<b>B<sub>1</sub></b>	<b>C<sub>1</sub></b>	<b>D<sub>1</sub></b>	<b>E<sub>1</sub></b>	<b>F<sub>1</sub></b>	<b>G<sub>1</sub></b>	<b>H<sub>1</sub></b>
<b>S</b> = 1	$x_0 y_1$	$x'_0 y'_1$	$x_1 y_0$	$x'_1 y'_0$	$x_2 y_3$	$x'_2 y'_3$	$x_3 y_2$	$x'_3 y'_2$
<b>M</b>	-2	-1	0	-1	0	1	0	-1
<b>A</b>	$(-\frac{5}{8}, -\frac{9}{8})$	$(-\frac{5}{8}, -\frac{9}{8})$	$(-\frac{5}{8}, -\frac{1}{8})$	$(-\frac{5}{8}, -\frac{1}{8})$	$(-\frac{5}{8}, -\frac{1}{8})$	$(\frac{3}{8}, -\frac{1}{8})$	$(\frac{3}{8}, -\frac{1}{8})$	$(-\frac{5}{8}, -\frac{1}{8})$

Table 2: Generators of  $C(G_B)$  having spin degree 1.

	<b>A<sub>2</sub></b>	<b>B<sub>2</sub></b>	<b>C<sub>2</sub></b>	<b>D<sub>2</sub></b>	<b>E<sub>2</sub></b>	<b>F<sub>2</sub></b>	<b>G<sub>2</sub></b>	<b>H<sub>2</sub></b>
<b>S</b> = 2	$x_0y_2$	$x'_0y'_2$	$x_1y_1$	$x'_1y'_1$	$x_2y_0$	$x'_2y'_0$	$x_3y_3$	$x'_3y'_3$
<b>M</b>	$-\frac{7}{4}$	$-\frac{3}{4}$	$\frac{1}{4}$	$-\frac{3}{4}$	$\frac{1}{4}$	$-\frac{3}{4}$	$\frac{1}{4}$	$-\frac{3}{4}$
<b>A</b>	$(-\frac{3}{8}, -\frac{3}{8})$	$(-\frac{3}{8}, -\frac{3}{8})$	$(-\frac{3}{8}, -\frac{3}{8})$	$(-\frac{3}{8}, -\frac{3}{8})$	$(-\frac{3}{8}, -\frac{3}{8})$	$(-\frac{3}{8}, -\frac{3}{8})$	$(-\frac{3}{8}, -\frac{3}{8})$	$(-\frac{3}{8}, -\frac{3}{8})$

Table 3: Generators of  $C(G_B)$  having spin degree 2.

37

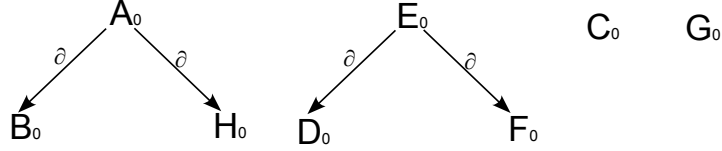
	<b>A<sub>3</sub></b>	<b>B<sub>3</sub></b>	<b>C<sub>3</sub></b>	<b>D<sub>3</sub></b>	<b>E<sub>3</sub></b>	<b>F<sub>3</sub></b>	<b>G<sub>3</sub></b>	<b>H<sub>3</sub></b>
<b>S</b> = 3	$x_0y_3$	$x'_0y'_3$	$x_1y_2$	$x'_1y'_2$	$x_2y_1$	$x'_2y'_1$	$x_3y_0$	$x'_3y'_0$
<b>M</b>	-2	-1	0	1	0	-1	0	-1
<b>A</b>	$(-\frac{9}{8}, -\frac{5}{8})$	$(-\frac{1}{8}, -\frac{5}{8})$	$(-\frac{1}{8}, \frac{3}{8})$	$(-\frac{1}{8}, \frac{3}{8})$	$(-\frac{1}{8}, -\frac{5}{8})$	$(-\frac{1}{8}, -\frac{5}{8})$	$(-\frac{1}{8}, -\frac{5}{8})$	$(-\frac{9}{8}, -\frac{5}{8})$

Table 4: Generators of  $C(G_B)$  having spin degree 3.

In order to compute  $H(C(G_B), \partial)$  we study four different cases, depending on the spin degree of the generators analyzed. Moreover we describe the behavior of the boundary operator using a diagram, with the following conventions

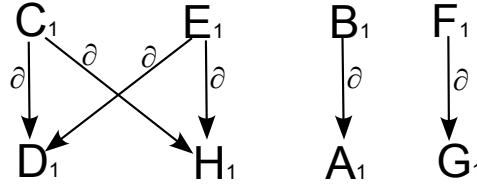
- if  $\partial(Z) = 0$ , no arrow will start from the generator  $Z$  of  $C(G_B)$ ;
- if  $\partial(Z) = Z_1 + \cdots + Z_k$  there will be an arrow starting from  $Z$  and ending in  $Z_i$ , for  $i = 1, \dots, k$ .

Let us start from spin degree 0. We have



so  $B_0, H_0, D_0, F_0, C_0$  and  $G_0$  are cycles and are not the boundary of any chain. The cycle  $B_0$  is equivalent to  $H_0$ , since their sum is the boundary of  $A_0$ , and, the same holds for  $D_0$  and  $F_0$ . Then  $B_0, C_0, G_0$  and  $D_0$  are the four generators of  $H(C(G_B), \partial)$  having spin degree equal to 0.

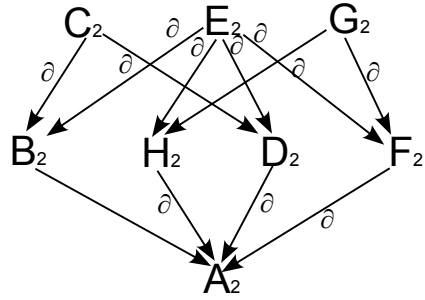
For spin degree 1 we have



so  $D_1$  (which is equivalent to  $H_1$ ) and  $C_1 + E_1$  are the two generators of  $H(C(G_B), \partial)$  having spin degree 1.

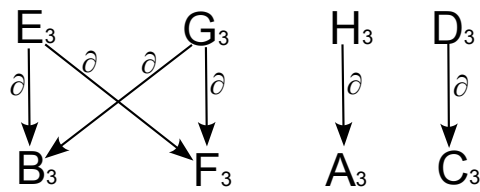


For spin degree 2 we get



so  $C_2 + E_2 + G_2$ ,  $B_2 + H_2$ ,  $B_2 + F_2$  and  $H_2 + D_2$  are the four generators of  $H(C(G_B), \partial)$  having spin degree 2.

Finally, for spin degree 3 we get



so  $B_3$  (which is equivalent to  $F_3$ ) and  $E_3 + G_3$  are the two generators of  $H(C(G_B), \partial)$  having spin degree 3.

According to Proposition 11, we have  $\widehat{HFL}(L_B) \cong H(C(G_B), \partial)$  and so

$$\begin{aligned} \widehat{HFL}(L_B) \cong & \mathbb{Z}_2 \left[ 0, \frac{1}{4}, \left( \frac{1}{8}, \frac{1}{8} \right) \right] \oplus \mathbb{Z}_2 \left[ 0, -\frac{3}{4}, \left( -\frac{7}{8}, \frac{1}{8} \right) \right] \oplus \mathbb{Z}_2 \left[ 0, -\frac{3}{4}, \left( \frac{1}{8}, -\frac{7}{8} \right) \right] \oplus \\ & \mathbb{Z}_2 \left[ 0, -\frac{7}{4}, \left( -\frac{7}{8}, -\frac{7}{8} \right) \right] \oplus \mathbb{Z}_2 \left[ 1, 0, \left( -\frac{5}{8}, -\frac{1}{8} \right) \right] \oplus \mathbb{Z}_2 \left[ 1, -1, \left( -\frac{5}{8}, -\frac{1}{8} \right) \right] \oplus \\ & \oplus \mathbb{Z}_2 \left[ 2, \frac{1}{4}, \left( -\frac{3}{8}, -\frac{3}{8} \right) \right] \oplus \mathbb{Z}_2 \left[ 2, -\frac{3}{4}, \left( -\frac{3}{8}, -\frac{3}{8} \right) \right]^3 \oplus \\ & \oplus \mathbb{Z}_2 \left[ 3, 0, \left( -\frac{1}{8}, -\frac{5}{8} \right) \right] \oplus \mathbb{Z}_2 \left[ 3, -1, \left( -\frac{1}{8}, -\frac{5}{8} \right) \right], \end{aligned}$$

where  $\mathbb{Z}_2[i, j, (k_1, k_2)]$  indicates a  $\mathbb{Z}_2$ -vector space generated by an element of spin degree  $i$ , Maslov degree  $j$  and Alexander bigrading  $(k_1, k_2)$ .

*Acknowledgments:* The authors are grateful to Chris Cornwell and Ken Baker for helpful discussions and to Ely Grigsby for a program computing HFK of knots in lens spaces with grid diagram at most two.

## References

- [BG] K. Baker, J. E. Grigsby, *Grid diagrams and Legendrian lens space links*, J. Symplectic Geom. **7** (2009), 415–448.
- [BGH] K. Baker, J. E. Grigsby, M. Hedden, *Grid diagrams for lens spaces and Combinatorial Knot Floer homology*, Int. Math. Res. Not. IMRN 2008 , Art. ID rnm024.
- [Be1] J. Berge, *Some knots with surgeries yielding lens spaces*, unpublished manuscript.
- [Be2] J. Berge, *The knots in  $D^2 \times S^1$  with non-trivial Dehn surgery yielding  $D^2 \times S^1$* , Topology Appl. **38** (1991), 1–19.
- [Br] H. Brunn, *Über verknötete Kurven*, Verhandlungen des Internationalen Math. Kongresses (1898), 256–259.

- [BM] D. Buck, M. Mauricio, *Connect sum of lens spaces surgeries: application to  $Hin$  recombination*, Math. Proc. Cambridge Philos. Soc. **150** (2011), 505–525.
- [CM] A. Cattabriga, M. Mulazzani,  *$(1,1)$ -knots via the mapping class group of the twice punctured torus*, Adv. Geom. **4** (2004), 263–277.
- [CMM] A. Cattabriga, E. Manfredi, M. Mulazzani, *On knots and links in lens spaces*, Topology Appl. **160** (2013), 430–442.
- [Co] C. Cornwell, *A polynomial invariant for links in lens spaces*, J. Knot Theory Ramifications **21** (2012), 1250060.
- [Cr] P. R. Cromwell, *Embedding knots and links in an open book I: Basic properties*, Topology Appl. **64** (1995), 37–58.
- [DL] I. Diamantis, S. Lambropoulou, *Braid equivalence in 3-manifolds with rational surgery description*, preprint, (2013), arXiv:1311.2465v1.
- [Dr] Y. V. Drobotukhina, *An analogue of the Jones polynomial for links in  $\mathbb{R}P^3$  and a generalization of the Kauffman-Murasugi theorem*, Leningrad Math. J. **2** (1991), 613–630.
- [Dy] I. A. Dynnikov, *Arc-presentations of links: monotonic simplification*, Fund. Math. **190** (2006), 29–76.
- [Gr] J. E. Greene, *The lens space realization problem*, Ann. of Math. **177** (2013), 449–511.
- [HL] V. Q. Huynh and T. T. Q. Le, *Twisted Alexander polynomial of links in the projective space*, J. Knot Theory Ramifications **17** (2008), 411–438.
- [La] S. Lambropoulou, *Solid torus links and Hecke algebras of  $\mathcal{B}$ -type*, Proc. Conf. Quant. Topology (1994), 225–245.

- [LR1] S. Lambropoulou, C. P. Rourke, *Markov theorem in 3-manifolds*, Topology Appl. **78** (1997), 95–122.
- [LR2] S. Lambropoulou, C. P. Rourke, *Algebraic Markov equivalence for links in three-manifolds*, Compos. Math. **142** (2006), 1039–1062.
- [Ma1] E. Manfredi, *Lift in the 3-sphere of knot and links in lens spaces*, preprint (2013), arXiv:1312.1256.
- [Ma2] E. Manfredi, *Knot and links in lens spaces*, Ph.D. thesis, in preparation.
- [MOS] C. Manolescu, P. Ozsváth, S. Sarkar, *A combinatorial description of knot Floer homology*, Ann. of Math. **169** (2009), 633–660.
- [Mr] M. Mroczkowski, *Polynomial invariants of links in the projective space*, Fund. Math. **184** (2004), 223–267.
- [OS] P. Ozsváth, Z. Szabò, *Holomorphic disks and topological invariants for closed three-manifolds*, Ann. of Math. **159** (2004), 1027–1158.
- [St] S. Stevan, *Torus Knots in Lens Spaces & Topological Strings*, preprint, (2013) arXiv:1308.5509.

ALESSIA CATTABRIGA, Department of Mathematics, University of Bologna, ITALY. E-mail: alessia.cattabriga@unibo.it

ENRICO MANFREDI, Department of Mathematics, University of Bologna, ITALY. E-mail: enrico.manfredi3@unibo.it

LORENZO RIGOLLI, Department of Mathematics, Ruhr University of Bochum, GERMANY. E-mail: Lorenzo.Rigolli@rub.de